

Supporting Information

Pushing to the Low Limits: Tetraazaanthracenes with Very Low-Lying LUMO Levels and Near-Infrared Absorption

Dominique Mario Gampe,^{1,†} Stefan Schramm,^{1,2,†} Florian Nöller,¹ Dieter Weiß,¹ Helmar Görls,³ Panče Naumov² and Rainer Beckert^{1,*}

¹ Friedrich Schiller University Jena, Institute of Organic and Macromolecular Chemistry, Humboldtstraße 10, 07743 Jena, Germany

² NYU Abu Dhabi, Saadiyat Campus, P.O. Box 129188, Abu Dhabi, United Arab Emirates

³ Friedrich Schiller University Jena, Institute of Inorganic and Analytical Chemistry, Humboldtstraße 8, 07743 Jena, Germany

* E-mail: rainer.beckert@uni-jena.de, Webpage: <http://www.agbeckert.uni-jena.de/>

† Both authors are contributed equally to this article.

Chemical Communications

Content

1. Experimental Procedures	2
1.1 General Procedures	2
1.2 Synthesis	2
2. Results and Discussion	6
2.1 Characterization of 11	6
2.2 Cyclo voltammograms of tetraazaanthracenes	8
2.3 Photostability	9
2.4 DFT calculations	12
3. Attachment	16
3.1 X-ray analysis	16
3.2 NMR spectra	18
4. References	26

1. Experimental Procedures

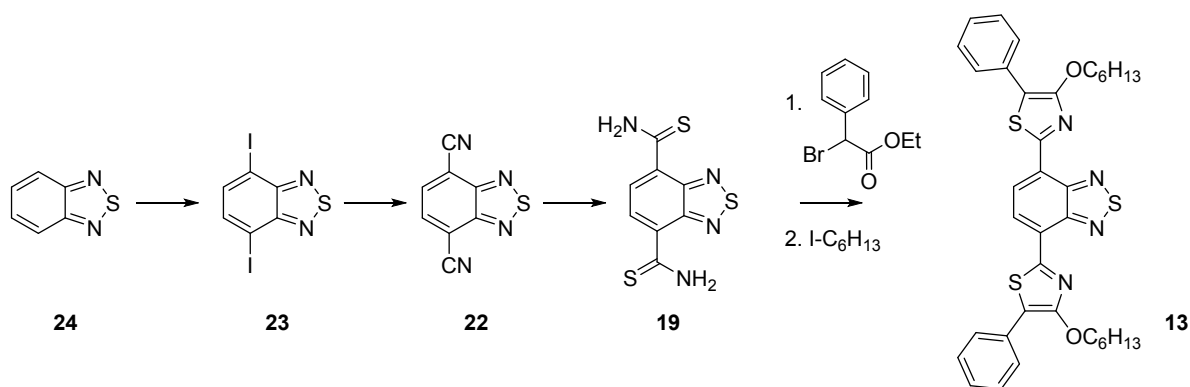
1.1 General Procedures

Solvents for UV-vis and emission spectroscopy were of analytical grade and purchased from Acros Organics. ^1H and ^{13}C NMR spectra were recorded on Bruker AC-250 (250 MHz), AC-300 (300 MHz) and AC-400 (400 MHz) spectrometers. Chemical shifts (δ) are given relative to solvents. Melting Points were determined under ambient conditions on a Galen III microscope from Cambridge Instruments equipped with a Lyca heating plate. UV-Vis data for the compounds were collected with a PerkinElmer LAMBDA 45 UV-vis spectrometer and emission spectra were measured with a Jasco FP 6500 instrument. Elemental analysis was carried out with a Leco CHNS- 932 instrument. Mass spectra were measured either with a Finnigan MAT SSQ 710 (EI) or a MAZ 95 XL (ESI) system. TLC materials were from Merck (Polygram SIL G/ UV254, aluminum oxide 60 F254). The material for column chromatography was also obtained from Merck (silica gel 60, 0,04 - 0,063 mm). The quantum yield of **11** were measured against fluorescein ($\Phi_{\text{F}} = 0.91 \text{ E mol}^{-1}$ in 1 M NaOH) as the fluorescence standard.¹ The cyclovoltammetric measurements were performed at a Metrohm Autolab PGSTAT30 potentiostat. in 0.1 M solution of TBAPF₆ in THF of spectroscopical grade (concentration of compounds: 1×10^{-5} M) on a glassy carbon working electrode with a scanning speed of 50 mV s^{-1} , platinum was used as counter and Ag/AgCl as the reference electrode. The data were calibrated externally versus ferrocene/ferrocenium. SEM was recorded on a FEI Quanta FEG 450 at 5 kV in high vacuum. The lyncée tec DHM®-R1000 with single laser source and stroboscopic module was used for holographical estimation of the layer thicknesses and the UV-vis transmission spectra were recorded on an Ocean Optics QE65 Pro using an Ocean Optics HL-2000 Halogen lightsource. The transmission spectra were corrected against the background noise, using the equation: Absorbance = $\log(I_0/I)$.

1.2 Synthesis

Ethyl 2-bromo-2-phenylacetate (**21**), ethyl 2-(benzo[c][1,2,5]thiadiazol-4-yl)-2-bromoacetate (**20**), 7-methylbenzo[c][1,2,5]thiadiazole-4-carbothioamide (**18**), pyridine-2-carbothioamide (**17**) and 4-(5-(benzo[c][1,2,5]thiadiazol-4-yl)-4-(hexyloxy)thiazol-2-yl)-7-methylbenzo[c][1,2,5]thiadiazole (**12**) were synthesized according to the literature.²

We used a slightly changed synthetic route for the synthesis of 4,7-bis(4-(hexyloxy)-5-phenylthiazol-2-yl)benzo[c][1,2,5]thiadiazole (**13**) (see Scheme S1). Instead of using 4,7-dibromobenzo[c][1,2,5]thiadiazole for the following Rosenmund-von-Braun reaction, to the dicyanide **22** as described in the literature, we attached two iodo-substituents to the thiazole (**23**). In consequence of the more reactive iodine-carbon bonding, the yield of the following nucleophilic substitution by means of CuCN (**22**) rose to 65%, the reaction time decreased to 1 h and we were able to perform the reaction in bigger batches (6 g instead of 1 g).



Scheme S1: Synthetic route to the dithiazolyl-substituted benzothiadiazol **13**.

*4,7-Diiodobenzo[c][1,2,5]thiadiazole (23)*³

Benzo[c][1,2,5]thiadiazole **24** (2.70 g, 19.9 mmol), iodine (16.10 g, 63.4 mmol) and Ag₂SO₄ (31.00 g, 100.1 mmol) were suspended in 80 mL of conc. H₂SO₄. The brown slurry was heated to 70 °C and stirred over 24 h, while the color changed to yellow and a white precipitate was formed. The resulting mixture was diluted with 300 mL water and the precipitate was filtrated. After rinsing with water, the precipitate was dried under reduced pressure and suspended in 100 mL toluene. Hot filtration of the latter, evaporation to approximately 20 mL and dilution with 20 mL of ethanol afforded the product as pale yellow crystals. After filtration of the product the crystals were rinsed with cold ethanol and dried to obtain **23** (5.70 g, 14.7 mmol, 75%). **M.p.:** 203-204 °C; **¹H NMR** (250 MHz, CDCl₃): δ = 7.81 (s, 2H) ppm; **¹³C NMR** (63 MHz, CDCl₃): δ = 154.0, 140.0, 87.9 ppm; **MS** (EI): m/z = 388 [M⁺]; **EA** calc. for C₆H₂I₂N₂S: C, 18.57; H, 0.52; N, 7.22; found: C, 18.81; H, 0.48; N, 7.13.

Benzo[c][1,2,5]thiadiazole-4,7-dicarbonitrile (22)

Compound **23** (6.01 g, 15.5 mmol) was dissolved in 30 mL *N*-methyl-2-pyrrolidone and purged with N₂ over 15 min. After heating of the solution to 80 °C, CuCN (4.21 g, 47.2 mmol, 3 equiv) was added carefully, while the reaction mixture turned to black and the temperature rose to approx. 120 °C. After stirring for 1 h at 150 °C the reaction was quenched by adding 15% NH₃-solution and extracted 4 times with ethyl acetate. The combined organic layers were dried over MgSO₄ and evaporated to dryness to obtain the crude brown product. Column chromatography (SiO₂; toluene; R_f ≈ 0.3) afforded the desired product **22** (1.89 g, 10.2 mmol, 65%). **M.p.:** 182-183 °C; **¹H NMR** (250 MHz, CDCl₃): δ = 8.13 (s, 2H) ppm; **¹³C NMR** (63 MHz, CDCl₃): δ = 152.6, 134.6, 114.0, 110.8 ppm; **MS** (EI): m/z = 186 [M⁺]; **EA** calc. for C₈H₂N₄S: C, 51.61; H, 1.08; N, 30.09; found: C, 51.93; H, 1.19; N, 30.21.

Benzo[c][1,2,5]thiadiazole-4,7-bis(carbothioamide) (**19**) and 4,7-bis(4-(hexyloxy)-5-phenylthiazol-2-yl)benzo[c][1,2,5]thiadiazole (**13**) were synthesized according to the literature obtaining slightly enhanced yields [2].

4-(4-(Hexyloxy)-2-(pyridin-2-yl)thiazol-5-yl)benzo[c][1,2,5]thiadiazole (11)

First reaction step: 0.72 g (5.2 mmol) of pyridine-2-carbothioamide (**17**), ethyl 2-(benzo[c][1,2,5]thiadiazol-4-yl)-2-bromoacetate (**20**; 2.41 g, 8.0 mmol) and sodium acetate (1.12 g, 13.6 mmol) were dissolved in 30 mL ethanol. The dark reaction mixture was heated to reflux with stirring for 6 h, while a red precipitate was formed. After hot filtration of the reaction mixture and rinsing of the precipitate with water, ethanol and *n*-pentane, the product was dried under reduced pressure and used as obtained without further purification.

The red 5-(benzo[*c*][1,2,5]thiadiazol-4-yl)-2-(pyridin-2-yl)thiazol-4-ol (0.93 g, 3.0 mmol) was suspended in 40 mL acetone, Na₂CO₃ (0.65 g, 6.1 mmol) and 1-iodohexane (0.48 mL, 0.7 g, 3.3 mmol) was added and the mixture was stirred under reflux for 24 h. The reaction was allowed to cool to room temperature and poured into 300 mL water. After extraction of the water phase with diethyl ether, the organic layer was dried over MgSO₄ and evaporated to dryness. Recrystallization from ethanol afforded the product as yellow crystals (0.99 g, 2.5 mmol, yield over two steps: 48%). **M.p.**: 104-105 °C; **¹H NMR** (250 MHz, CDCl₃): δ = 8.64 (dd, *J* = 4.8, 0.6 Hz, 1H), 8.51 (dd, *J* = 7.3, 0.7 Hz, 1H), 8.16 (d, *J* = 7.9 Hz, 1H), 7.84 (dd, *J* = 8.7, 0.7 Hz, 1H), 7.78 (td, *J* = 7.9, 1.8 Hz, 1H), 7.65 (dd, *J* = 8.7, 7.4 Hz, 1H), 7.30 (ddd, *J* = 7.5, 4.9, 1.0 Hz, 1H), 4.64 (t, *J* = 6.6 Hz, 2H), 2.01 – 1.86 (m, 2H), 1.62 – 1.49 (m, 2H), 1.47 – 1.31 (m, 4H), 0.92 (t, *J* = 7.0 Hz, 3H) ppm; **¹³C NMR** (63 MHz, CDCl₃): δ = 164.1, 162.4, 155.2, 152.5, 151.8, 149.7, 137.0, 130.2, 125.8, 125.7, 124.4, 119.3, 119.0, 109.6, 70.9, 31.7, 29.7, 26.0, 22.8, 14.2 ppm; **MS** (ESI-pos): *m/z* = 419.1 [(M+Na)⁺]; **HRMS** (ESI-pos): calc.: 419.0976, found: 419.0979; **EA** calc. for C₂₀H₂₀N₄OS₂: C, 60.58; H, 5.08; N, 14.13; found: C, 60.33; H, 5.15; N, 14.28.

*6-(4-(Hexyloxy)-2-(pyridin-2-yl)thiazol-5-yl)-5,10-dihydropyrazino[2,3-*b*]quinoxaline-2,3-dicarbonitrile (4)*

0.50 g (1.3 mmol) of compound **11** were dissolved in 20 mL of a mixture of ethanol/THF (3:1) and purged with N₂ for 15 min. NaBH₄ (0.43 g, 11.3 mmol, 9 equiv) and a spatula of CoCl₂ was added carefully before the resulting mixture was stirred under reflux and N₂. The reaction was allowed to cool to room temperature, when everything of **11** was consumed (TLC: SiO₂; toluene/ethyl acetate, 5:1; educt: *R_f* ≈ 0.8, product: *R_f* ≈ 0.2). The mixture was evaporated and the residue was dissolved in water and diethyl ether. After triple extraction of the water phase with diethyl ether, the organic phases were combined, dried over MgSO₄ and evaporated to dryness, to afford the crude diamine **8** as pale yellow oil, which was used as obtained for the following cyclization reaction. Therefore **8** was dissolved in 10 mL of dry dioxane and 5,6-dichloropyrazine-2,3-dicarbonitrile (**7**; 0.25 g, 1.3 mmol) was added under nitrogen. The resulting reaction mixture was stirred under reflux and N₂ for 5 h and at 80 °C overnight, while an orange precipitate was formed. Filtration of the mixture and rinsing with water, ethanol and *n*-pentane afforded the brown product (0.20 g, 0.4 mmol, 32%). **M.p.**: 252-253 °C; **¹H NMR** (250 MHz, THF-*d*8): δ = 9.45 (s, 1H), 8.54 (d, *J* = 4.5 Hz, 1H), 8.30 (s, 1H), 8.09 (d, *J* = 7.9 Hz, 1H), 7.84 (td, *J* = 7.7, 1.5 Hz, 1H), 7.36 (dd, *J* = 7.0, 5.2 Hz, 1H), 6.73 – 6.58 (m, 2H), 6.36 (dd, *J* = 5.8, 3.2 Hz, 1H), 4.48 (t, *J* = 6.6 Hz, 2H), 1.92 – 1.78 (m, 2H), 1.56 – 1.44 (m, 2H), 1.42 – 1.29 (m, 4H), 0.92 (t, *J* = 6.9 Hz, 3H) ppm; **¹³C NMR** (63 MHz, THF-*d*8): δ = 165.4, 159.9, 152.0, 150.6, 148.2, 148.0, 137.9, 132.1, 129.3, 127.7, 125.55, 125.1, 124.6, 119.4, 118.2, 115.3, 115.3, 114.9, 108.6, 71.7, 32.7, 30.4, 26.7, 23.6, 14.5 ppm; **MS** (EI): *m/z* = 494 [M⁺]; **EA** calc. for C₂₆H₂₂N₈OS: C, 63.14; H, 4.48; N, 22.66; found: C, 63.49; H, 4.56; N, 22.38.

*6-(5-(2,3-Dicyano-5,10-dihydropyrazino[2,3-*b*]quinoxalin-6-yl)-4-(hexyloxy)thiazol-2-yl)-9-methyl-5,10-dihydropyrazino[2,3-*b*]quinoxaline-2,3-dicarbonitrile (5)*

0.50 g (1.1 mmol) of compound **12** were dissolved in 40 mL of a mixture of ethanol/THF (3:1) and purged with N₂ for 15 min. NaBH₄ (0.73 g, 19.2 mmol, 18 equiv) and a spatula of CoCl₂ was added carefully before the resulting mixture was stirred under reflux and N₂. The reaction was allowed to cool to room temperature, when everything of **12** was consumed (TLC: SiO₂; toluene/ethyl acetate, 2:1; educt: *R_f* ≈ 0.9, product: *R_f* ≈ 0.2). The mixture was evaporated and the residue was dissolved in water and diethyl ether. After triple extraction of the water phase with diethyl ether, the organic phases were combined, dried over MgSO₄ and evaporated to dryness, to afford the crude *bis*-diamine **9** as pale yellow oil, which was used as obtained for the following cyclization reaction. Therefore **9** was dissolved in 10 mL of dry dioxane and 5,6-dichloropyrazine-2,3-dicarbonitrile (**7**; 0.42 g, 2.1 mmol)

was added under nitrogen. The resulting reaction mixture was stirred under reflux and N₂ for 24 h, while an orange precipitate was formed. Filtration of the mixture and rinsing with water, ethanol and *n*-pentane afforded the brown product (0.41 g, 0.6 mmol, 58%). **M.p.**: >360 °C; **¹H NMR** (400 MHz, DMSO-*d*₆): δ = 10.99 (s, 1H), 10.42 (s, 1H), 9.77 (s, 1H), 9.17 (s, 1H), 6.93 (d, *J* = 8.2 Hz, 1H), 6.65 (t, *J* = 7.4 Hz, 1H), 6.61 – 6.51 (m, 2H), 6.45 (d, *J* = 7.7 Hz, 1H), 4.23 (t, *J* = 6.8 Hz, 2H), 3.57 (s, 3H), 1.77 – 1.69 (m, 2H), 1.44 – 1.37 (m, 2H), 1.34 – 1.28 (m, 4H), 0.88 (t, *J* = 6.4 Hz, 3H) ppm; **¹³C NMR** could not be measured due to bad solubility; **MS** (EI): *m/z* = 663 [M⁺]; **EA** calc. for C₃₄H₂₅N₁₃OS: C, 61.53; H, 3.80; N, 27.43; found: C, 61.82; H, 3.71; N, 27.67.

*6,9-Bis(4-(hexyloxy)-5-phenylthiazol-2-yl)-5,10-dihydropyrazino[2,3-*b*]quinoxaline-2,3-dicarbonitrile (6)*

0.31 g (0.5 mmol) of compound **13** were dissolved in 40 mL of a mixture of ethanol/THF (3:1) and purged with N₂ for 15 min. NaBH₄ (0.16 g, 4.2 mmol, 9 equiv) and a spatula of CoCl₂ was added carefully before the resulting mixture was stirred under reflux and N₂. The reaction was allowed to cool to room temperature, when everything of **13** was consumed (TLC: SiO₂; toluene; educt: R_f ≈ 0.9, product: R_f ≈ 0.3). The mixture was evaporated and the residue was dissolved in water and diethyl ether. After triple extraction of the water phase with diethyl ether, the organic phases were combined, dried over MgSO₄ and evaporated to dryness, to afford the crude diamine **10** as brown glassy solid, which was used as obtained for the following cyclization reaction. Therefore **10** was dissolved in 20 mL of dry dioxane and 5,6-dichloropyrazine-2,3-dicarbonitrile (**7**; 0.09 g, 0.5 mmol) was added under nitrogen. The resulting reaction mixture was stirred under reflux and N₂ for 6 h and at 80 °C overnight, while an orange precipitate was formed. Evaporation to approx. 10 mL, filtration of the mixture and rinsing with water, ethanol and *n*-pentane afforded the red product (0.12 g, 0.2 mmol, 33%). **M.p.**: 280 °C (dec.); **¹H NMR** (250 MHz, CDCl₃): δ = 11.43 (s, 2H), 7.71 (d, *J* = 7.7 Hz, 4H), 7.38 (t, *J* = 7.6 Hz, 4H), 7.29 (d, *J* = 4.9 Hz, 2H), 6.97 (s, 2H), 4.37 (t, *J* = 6.7 Hz, 4H), 1.90 – 1.81 (m, 4H), 1.51 – 1.47 (m, 4H), 1.39 – 1.33 (m, 8H), 0.91 (t, *J* = 6.9 Hz, 6H) ppm; **¹³C NMR** could not be measured due to bad solubility; **MS** (EI): *m/z* = 752 [M⁺]; **EA** calc. for C₄₂H₄₀N₈O₂S₂: C, 67.00; H, 5.35; N, 14.88; found: C, 67.35; H, 5.21; N, 14.66.

*6-(4-(Hexyloxy)-2-(pyridin-2-yl)thiazol-5-yl)pyrazino[2,3-*b*]quinoxaline-2,3-dicarbonitrile (1)*

0.10 g (0.2 mmol) of dihydroanthracene **4** were dissolved in 10 mL of dry and purged THF and 0.05 g (0.2 mmol, 1.1 equiv) of 2,3-Dichloro-5,6-dicyano-1,4-benzoquinone (DDQ) were added, while the mixture turned to black. After stirring under N₂ for 24 h, the reaction was quenched by adding 50 mL water and a blue, crystalline precipitate was formed and filtrated. Washing of the precipitate intensively with water and drying of the microcrystals afforded target product **1** in 91% yield (0.09 g, 0.2 mmol). **M.p.**: 269-270 °C; **¹H NMR** (250 MHz, THF-*d*₈): δ = 9.13 (dd, *J* = 5.2, 3.5 Hz, 1H), 8.67 (d, *J* = 4.4 Hz, 1H), 8.30 – 8.21 (m, 2H), 8.18 (d, *J* = 7.8 Hz, 1H), 7.88 (t, *J* = 7.0 Hz, 1H), 7.41 (dd, *J* = 7.0, 5.0 Hz, 1H), 4.74 (t, *J* = 6.6 Hz, 2H), 2.05 – 1.92 (m, 2H), 1.68 – 1.55 (m, 2H), 1.49 – 1.35 (m, 4H), 0.94 (t, *J* = 6.9 Hz, 3H) ppm; **¹³C NMR** (63 MHz, THF-*d*₈): δ = 170.4, 168.0, 164.2, 152.6, 150.7, 149.1, 145.4, 143.8, 142.3, 137.8, 136.8, 136.6, 136.0, 134.1, 131.8, 128.1, 125.63, 119.8, 114.5, 108.4, 71.7, 32.6, 30.5, 26.8, 23.6, 14.4 ppm; **MS** (EI): *m/z* = 492 [M⁺]; **HRMS** (EI): calc.: 492.1481, found: 492.1482; **EA** calc. for C₂₆H₂₀N₈OS: C, 63.40; H, 4.09; N, 22.75; found: C, 63.71; H, 4.12; N, 22.62.

*6-(5-(2,3-Dicyanopyrazino[2,3-*b*]quinoxalin-6-yl)-4-(hexyloxy)thiazol-2-yl)-9-methylpyrazino[2,3-*b*]quinoxaline-2,3-dicarbonitrile (2)*

0.10 g (0.2 mmol) of *bis*-dihydroanthracene **5** were dissolved in 10 mL of dry and purged THF and 0.08 g (0.3 mmol, 2.2 equiv) of DDQ were added, while the mixture turned to dark green. After stirring under N₂ for 48 h, the reaction mixture was poured in 100 mL water and a green precipitate was formed and filtrated. The precipitate was washed intensively with water (approx. 1 L) and dried under reduced pressure. Column chromatography (SiO₂; toluene/ethyl acetate: 10/1; R_f ≈ 0.5) was carried out to obtain the desired product **2** as green powder (0.06 g, 0.1 mmol, 57%). **M.p.**: >360 °C; **¹H NMR** (400 MHz, THF-d₈): δ = 9.10 (d, *J* = 7.3 Hz, 1H), 8.98 (dd, *J* = 6.9, 1.5 Hz, 1H), 8.33 (dd, *J* = 8.7, 1.6 Hz, 1H), 8.31 – 8.27 (m, 1H), 8.18 (d, *J* = 7.4 Hz, 1H), 4.78 (t, *J* = 6.6 Hz, 2H), 3.03 (s, 3H), 2.03 – 1.96 (m, 2H), 1.65 – 1.59 (m, 2H), 1.47 – 1.39 (m, 4H), 0.94 (t, *J* = 7.1 Hz, 3H) ppm; **¹³C NMR** (101 MHz, THF-d₈): δ = 163.4, 159.7, 148.9, 148.0, 145.8, 145.6, 144.0, 142.9, 141.4, 136.9, 136.8, 136.8, 136.5, 136.1, 135.0, 134.1, 133.7, 132.9, 131.8, 128.7, 114.5, 114.5, 111.2, 79.7, 79.3, 79.0, 71.5, 32.6, 30.5, 26.9, 23.6, 18.0, 14.5 ppm; **MS** (EI): *m/z* = 660 [M⁺]; **HRMS** (EI) could not be measured, substance does not vaporize until 340 °C and no signals could be detected *via* ESI-MS; **EA** calc. for C₃₄H₂₁N₁₃OS: C, 61.90; H, 3.21; N, 27.60; found: C, 62.12; H, 3.32; N, 27.81.

6,9-Bis(4-(hexyloxy)-5-phenylthiazol-2-yl)pyrazino[2,3-b]quinoxaline-2,3-dicarbonitrile (3)

0.10 g (0.1 mmol) of *bis*-thiazole **6** were dissolved in 10 mL of dry and purged THF and 0.03 g (0.1 mmol, 1.1 equiv) of DDQ were added, while the mixture turned to black. After stirring under N₂ for 24 h, the reaction was quenched by adding 50 mL water and a dark yellow precipitate was formed and filtrated. Washing of the precipitate intensively with water (approx. 500 mL) and drying under reduced pressure afforded the crude target product. Column chromatography (SiO₂; CHCl₃; R_f ≈ 0.5) was carried out to obtain the desired product **3** as yellow-brown powder (0.09 g, 0.1 mmol, 90%). **M.p.**: 204-206 °C; **¹H NMR** (250 MHz, CDCl₃): δ = 8.17 (s, 2H), 7.48 (d, *J* = 6.8 Hz, 4H), 7.39 – 7.28 (m, 6H), 3.97 (t, *J* = 5.1 Hz, 4H), 1.71 – 1.60 (m, 4H), 1.26 – 1.18 (m, 12H), 0.81 (t, *J* = 6.2 Hz, 6H) ppm; **¹³C NMR** (63 MHz, CDCl₃): δ = 159.2, 150.1, 142.8, 140.1, 133.9, 130.7, 130.5, 130.2, 129.3, 128.0, 126.3, 118.0, 112.3, 70.7, 31.8, 29.6, 25.9, 22.8, 14.1 ppm; **MS** (EI): *m/z* = 750 [M⁺]; **HRMS** (EI): calc.: 750.2559, found: 750.2546; **EA** calc. for C₄₂H₃₈N₈O₂S₂: C, 67.18; H, 5.10; N, 14.92; found: C, 67.42; H, 5.14; N, 14.81.

2. Results and Discussion

2.1 Characterization of **11**

Additionally to the characterization of the D-A- type target compounds bearing tetraazaanthracenes as the accepting moiety, we characterized 4-(4-(Hexyloxy)-2-(pyridin-2-yl)thiazol-5-yl)benzo[c][1,2,5]thiadiazole (**11**) by means of UV/Vis absorption and fluorescence emission spectroscopy as well as cyclic voltammetric measurements. All measurements were carried out in THF. The photochemical spectra are depicted in Figure S1 and the cyclic voltammogram is depicted in Figure S2. Derivative **11** exhibits four major absorption bands with maxima at: λ (ε) = 242 (2.48 · 10⁴ M⁻¹cm⁻¹), 323 (1.64 · 10⁴ M⁻¹cm⁻¹), 363 (1.40 · 10⁴ M⁻¹cm⁻¹) and 433 nm (1.93 · 10⁴ M⁻¹cm⁻¹). The maximum of the yellow fluorescence is located at 543 nm and a fluorescence quantum yield of 0.22 was observed in THF. The optical bandgap was estimated to 2.52 eV. In the reduction cycle of the cyclic voltammogram, **11** shows two reversible reduction waves at half step potentials of -1.9 V (which is attributed to the benzothiadiazole unit) and -2.5 V, which we assign to the pyridyl moiety.

An irreversible oxidation peak at approximately 1 V can be observed within the oxidation cycle of **11**, which is typical for 4-alkoxythiazols. *Via* the onset values, the HOMO and LUMO can be estimated to -5.83 and -3.28 eV and the electrochemical bandgap of 2.55 eV fits perfectly with the optical bandgap.

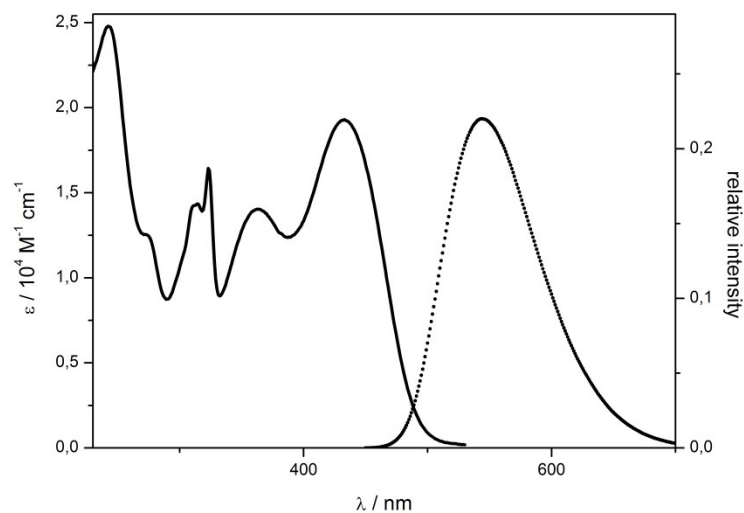


Figure S1 UV-Vis absorption (solid line) and fluorescence emission (dotted line) spectra of derivative **11**.

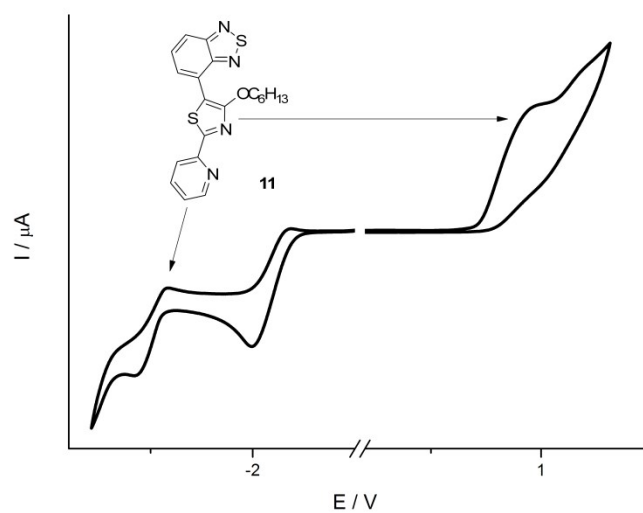


Figure S2 Cyclovoltammogram of derivative **11**, calibrated externally against Fc/Fc^+ .

2.2 Cyclo voltammograms of tetraazaanthracenes

The cyclo voltammograms of the three tetraazaanthracene derivatives (**1**, **2**, **3**) are shown in Figure S3, Figure S4 and Figure S5.

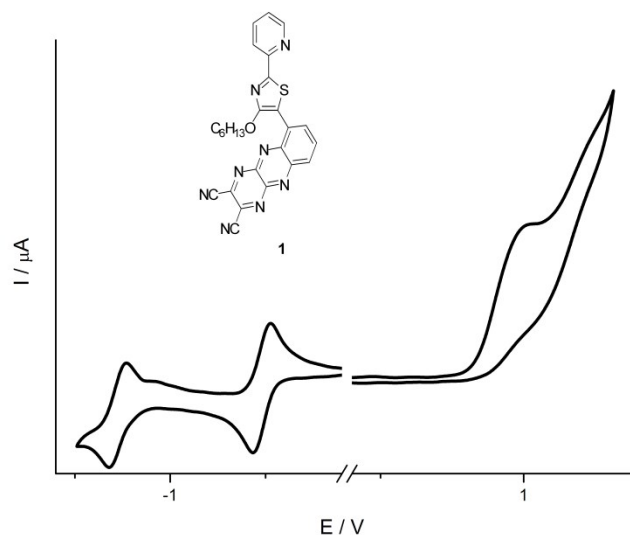


Figure S3 Cyclovoltammogram of target compound **1**, externally calibrated against Fc/Fc⁺.

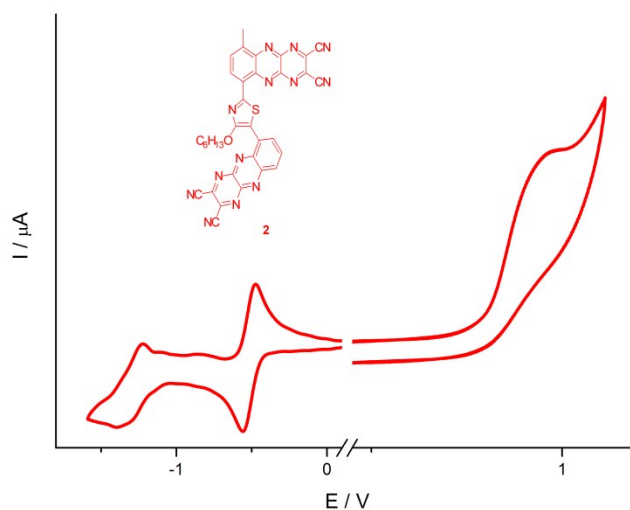


Figure S4 Cyclovoltammogram of target compound **2**, externally calibrated against Fc/Fc⁺.

Due to the asymmetric substitution of the two anthracene moieties in **2** (one bearing a methyl-residue and 5- or 2-thiazolyl-residue) the respectively second reduction steps occur at slightly different potentials. It can be assumed that the first reduction (-0.52 V) occurs at the outer pyrazine ring and the second reduction (~ -1.31 V) at the mid-position of the anthracenes, because of the more pronounced asymmetry.

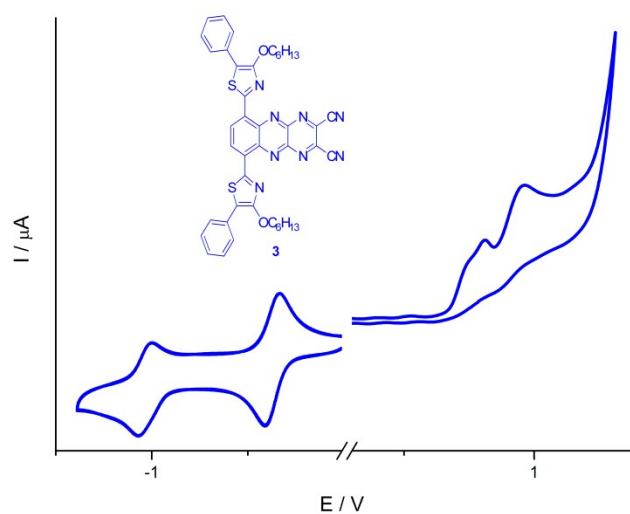


Figure S5 Cyclic voltammogram of target compound **3**, externally calibrated against Fc/Fc⁺.

2.3 Photostability

To investigate the photostability, we measured the UV-vis spectra of the anthracenes. The compounds were dissolved in THF of spectroscopical grade. Solutions were exposed under irradiation of a 150 W Xenon lamp at 680 nm (**1**, **2**) and 830 nm (**3**), respectively, over 5 min. After these 5 min a spectrum was measured, and the substances were again exposed for 5 min. The legends indicate the pure exposure time. During these measurements, the absorbances decrease only slightly, which points to high photostabilities of the target compounds.

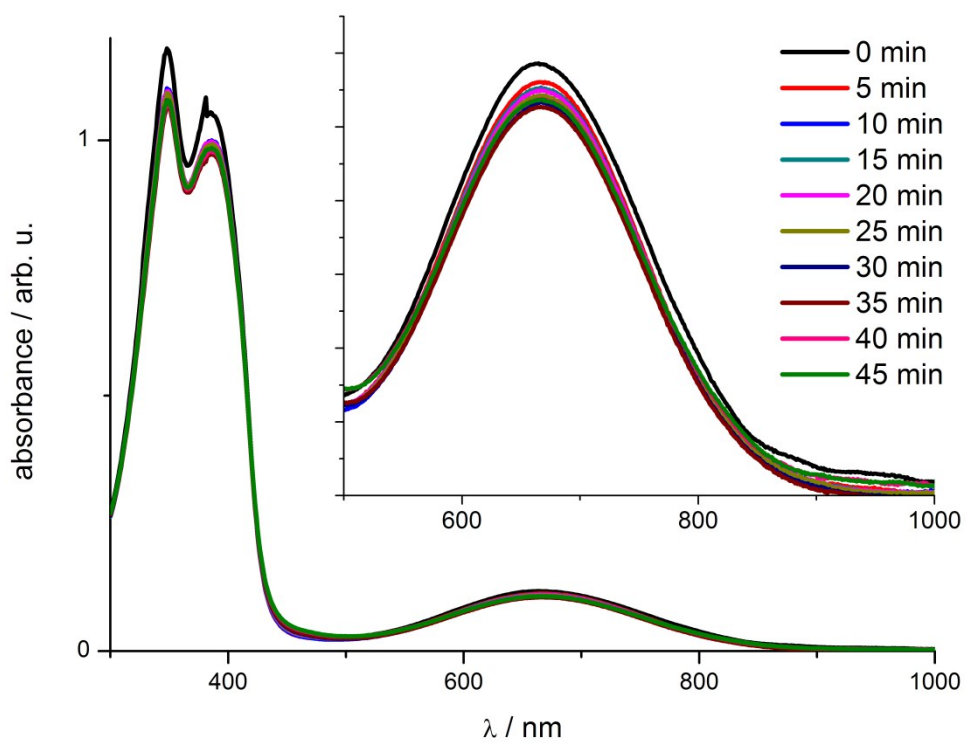


Figure S6 Photostability measurement of 1.

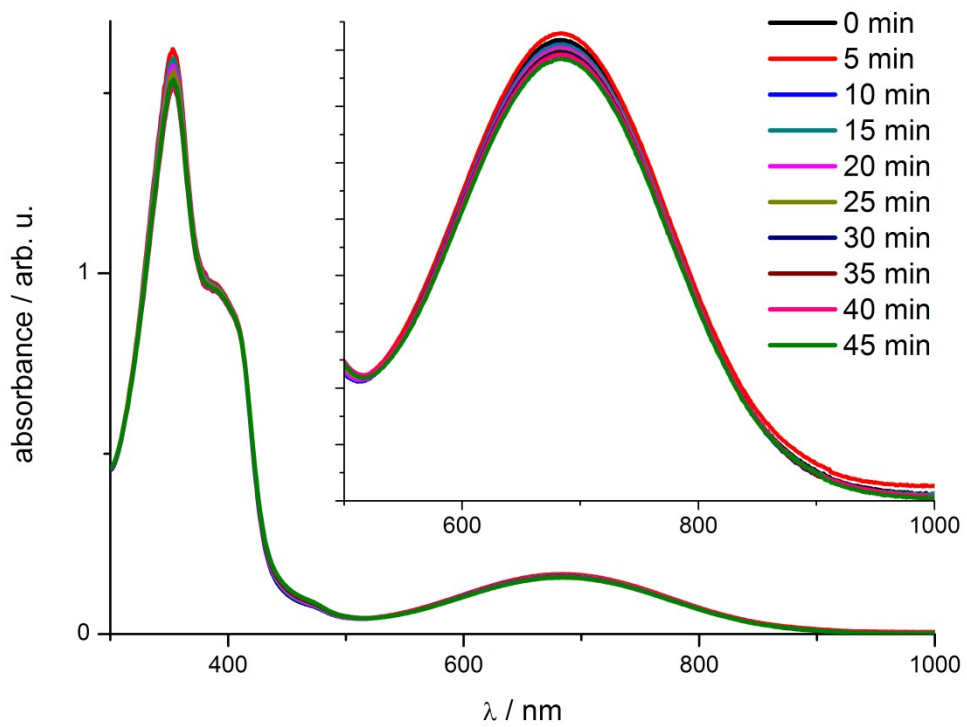


Figure S7 Photostability of 2.

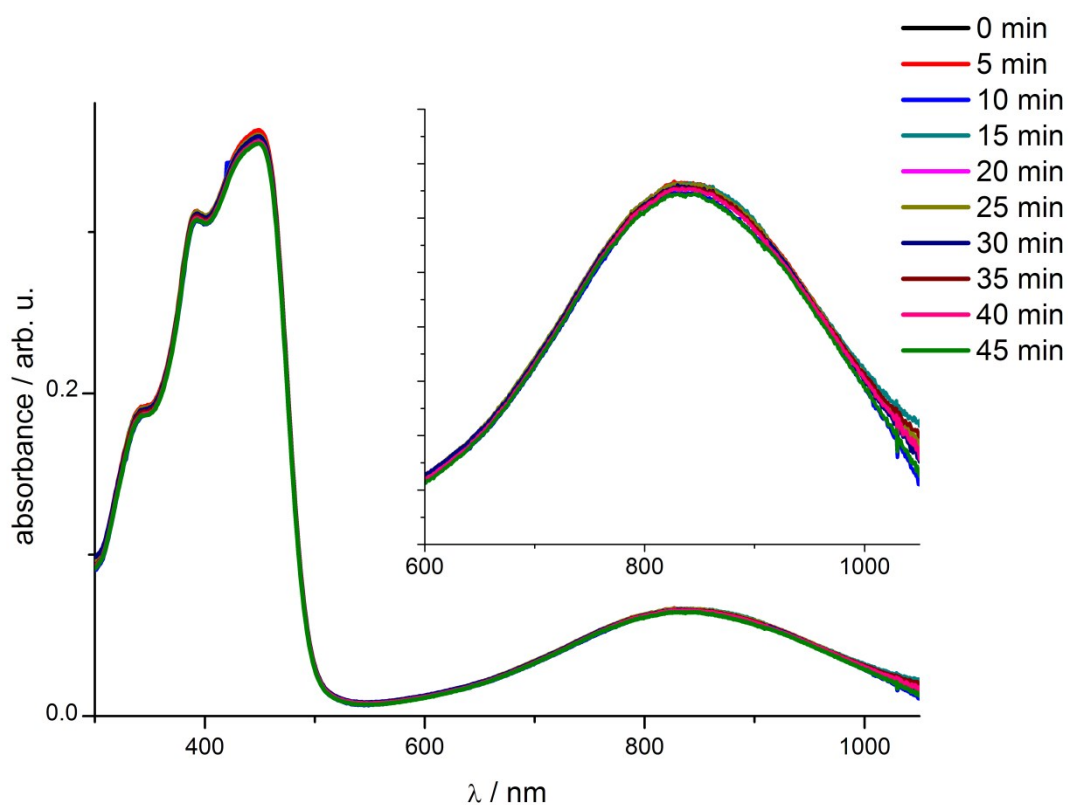


Figure S8 Photostability measurement of **3**.

Additionally we measured long-term photostability of compound **1**. The same equipment as described above was used. The solution was irradiated over 24 h, while every hour a spectrum was measured over the first 4 and the last 4 hours. See Figure S9 for the photochemical decomposition of **1** in THF at 10 °C.

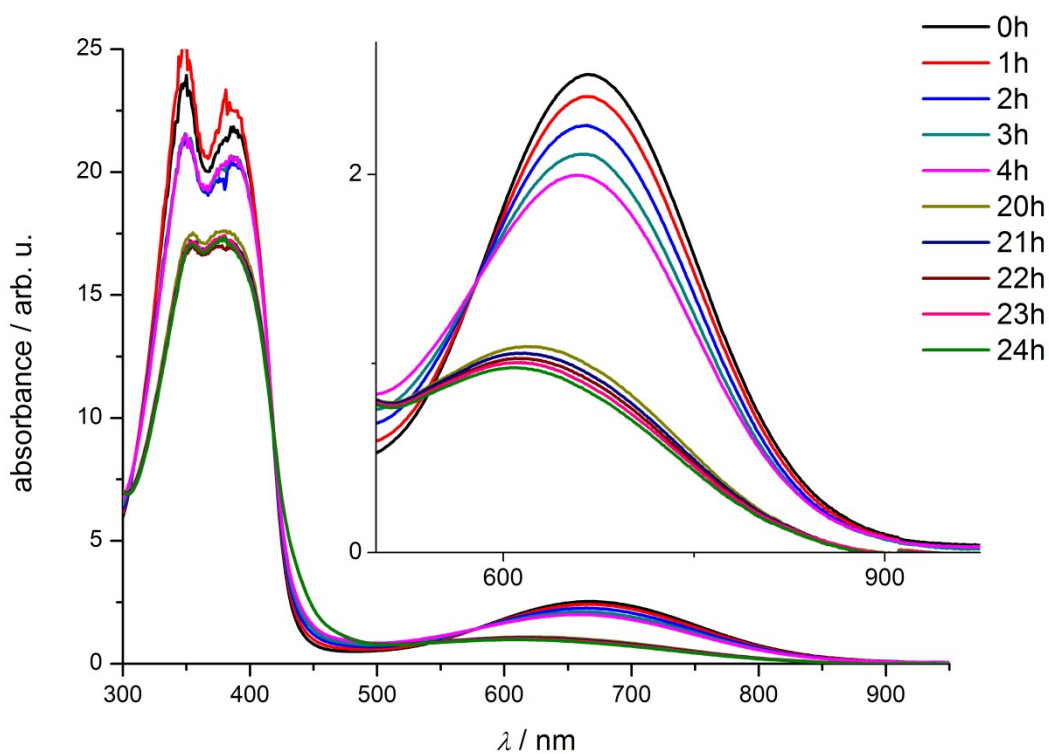


Figure S9 Long-term stability test of compound **1**.

The absorbance decrease at 666 nm was used for the decomposition. Via the molar extinction coefficient the concentration was estimated and plotted against the time (see Figure S10). Via an exponential fit we obtained the decomposition coefficient ($k = 2.24 \pm 0.12 \cdot 10^{-5} \text{ s}^{-1}$) and were able to calculate the photochemical half-life via the equation: $T_{1/2} = \ln(2) / k = 30899 \pm 1826 \text{ s}$.

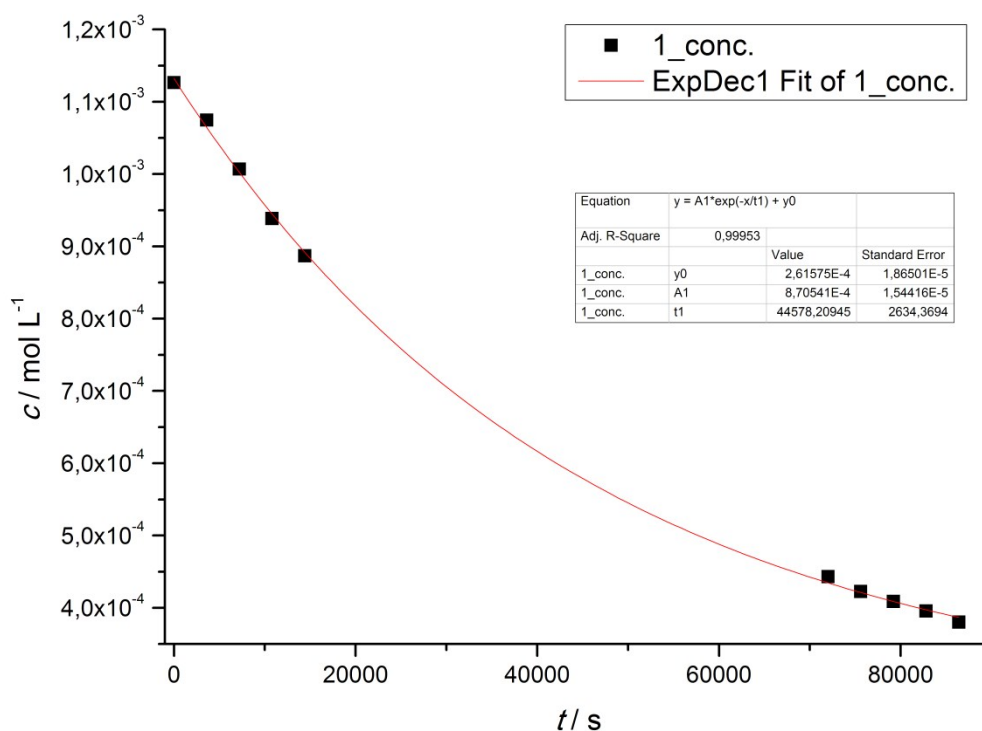


Figure S10 Exponential fit of the concentration over time plot (t1 is the reciprocal decomposition coefficient).

2.4 Film UV-vis

1 mg of each compound was dissolved in 100 μl HPLC pure THF and sonicated for 5 min. 30 μl of each sample was drop casted on a previously cleaned microscopic slide. After the complete evaporation of the solvent (1.5 h) the UV-vis transmission spectra were measured (see Figure S14, Figure S15 and Figure S16), corrected and the structure of the films were investigated using SEM. For the reason of conductivity, the samples were sputter coated with a gold film of about 5-10 nm.

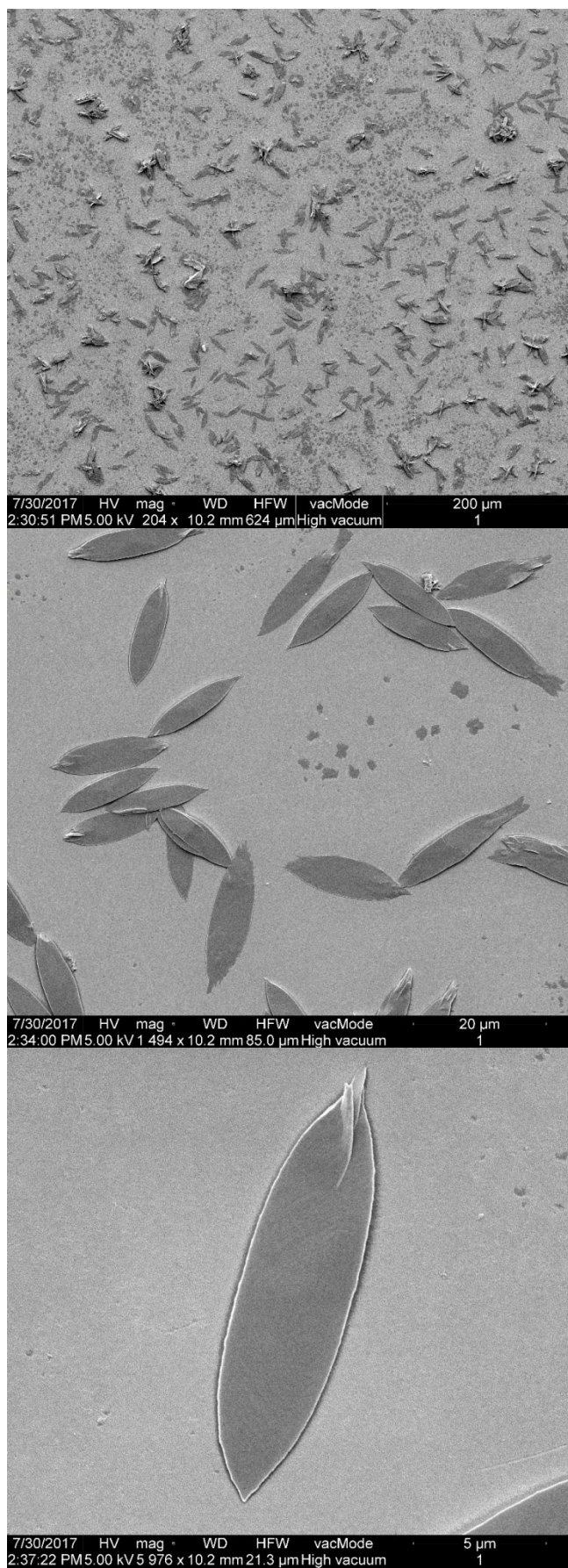


Figure S11 SEM images of film, formed from compound **1**. Material **1** does not form clean films but forms micro/nano crystals when drop casted under the described conditions.

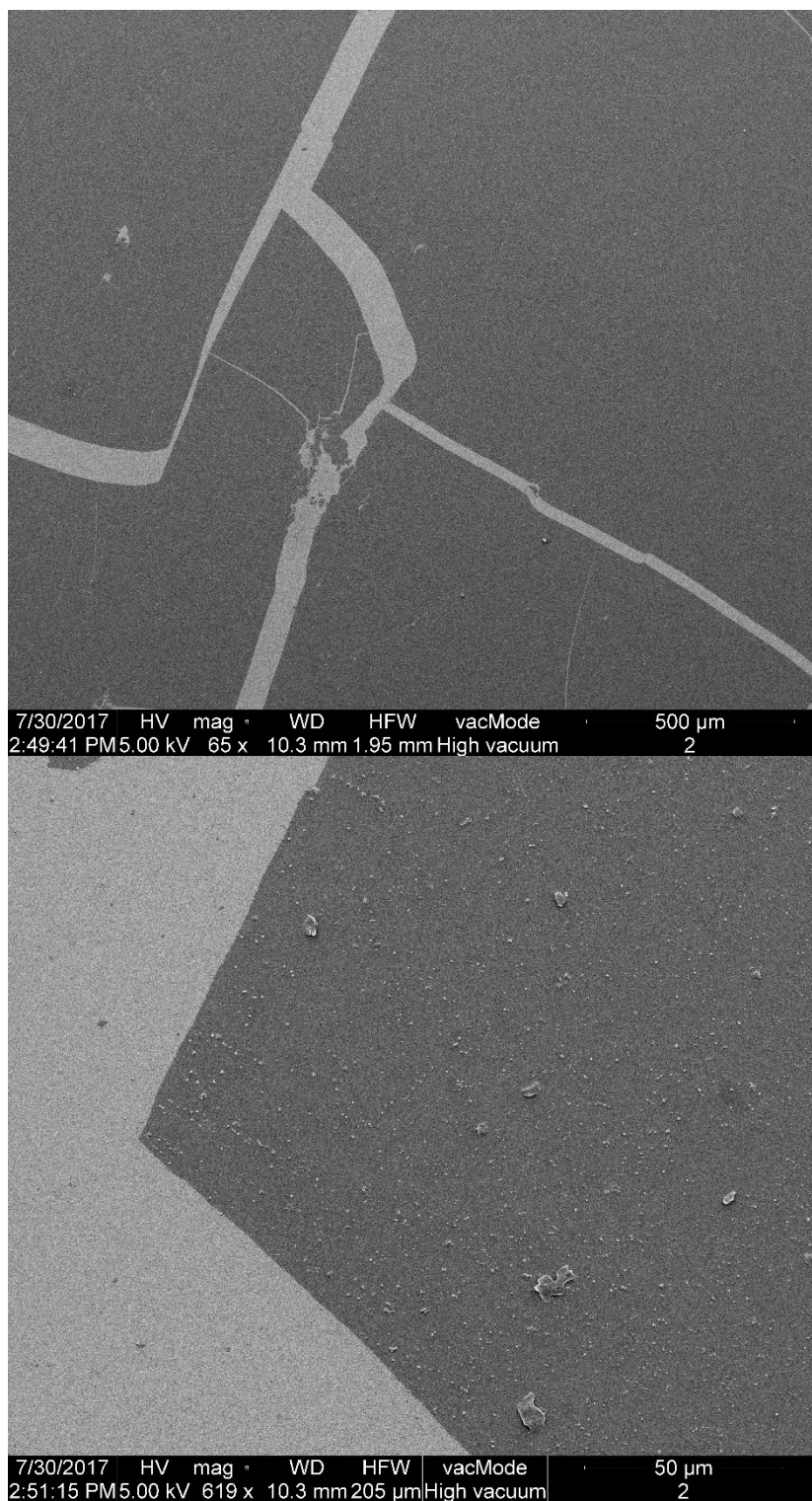


Figure S12 SEM images of compound **2**. It forms very clean films that seem to crack due to the fast evaporation of the solvent. Bottom picture: left: clean, right: film.

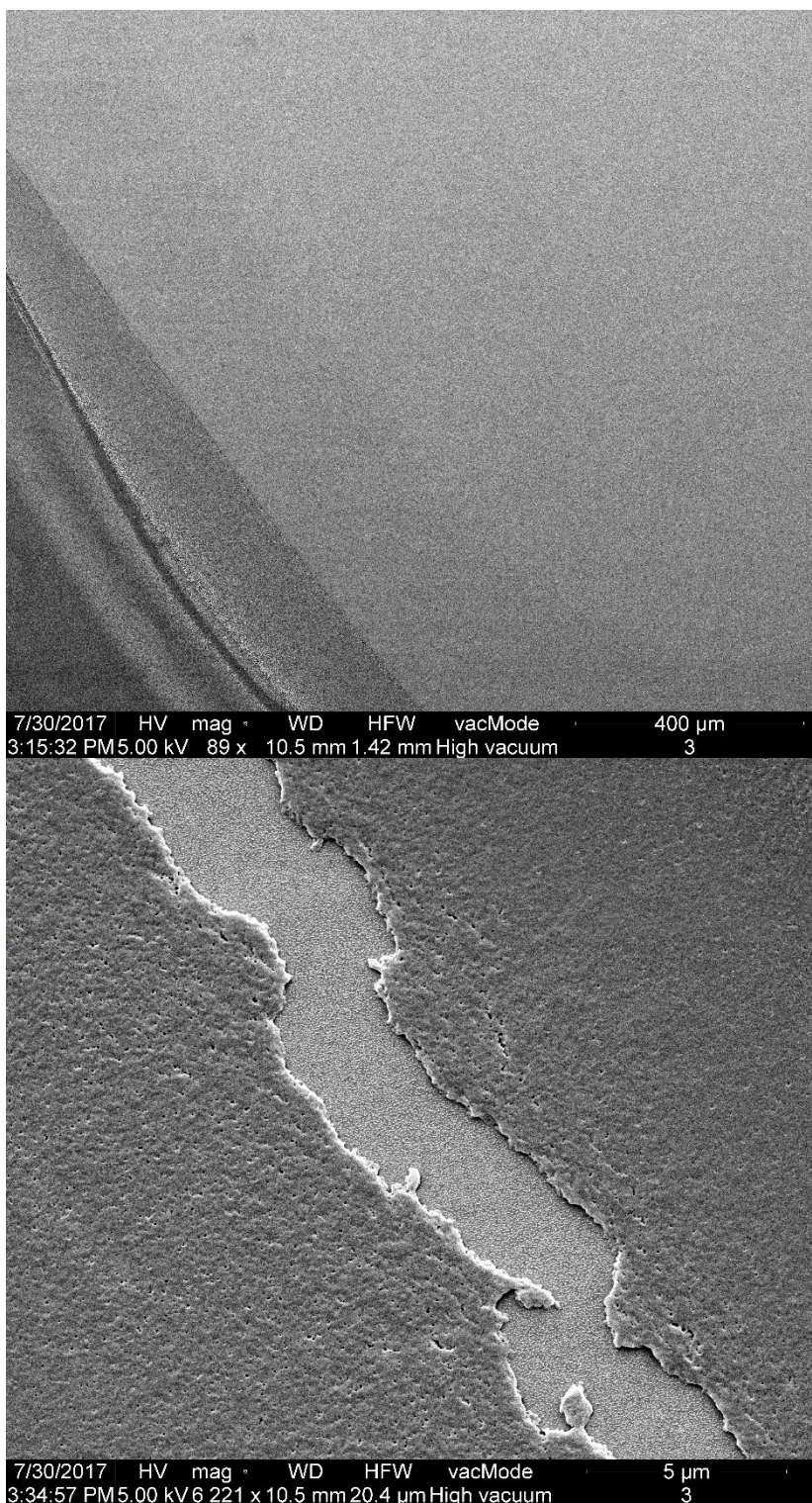


Figure S13 SEM images of compound **3**. Compound **3** forms films but they do not have a as clean surface as **2**. They seem to have a nano structured surface. Bottom picture: middle: clean, left and right: film.

After this the layer thicknesses of the films were measured using holographic microscopy. All films have within the error of the measurement a thickness of 40-50 nm. The dataset for **2** is shown exemplarily below (Figure S12 and Figure S13).

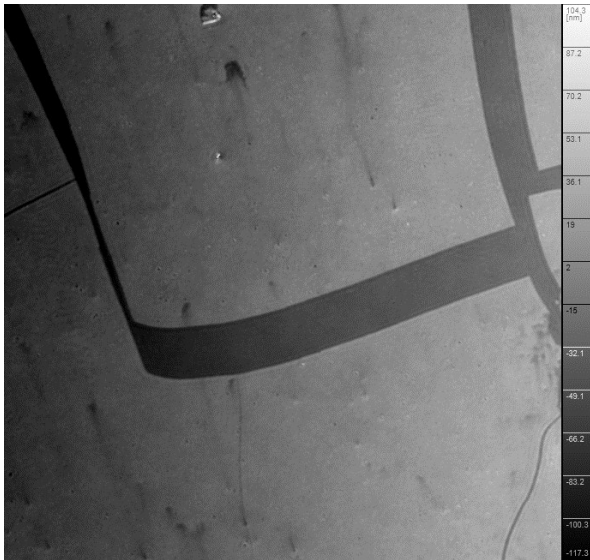


Figure S14 Reconstructed hologram of the film surface of 2. Bright: film, dark: clean.

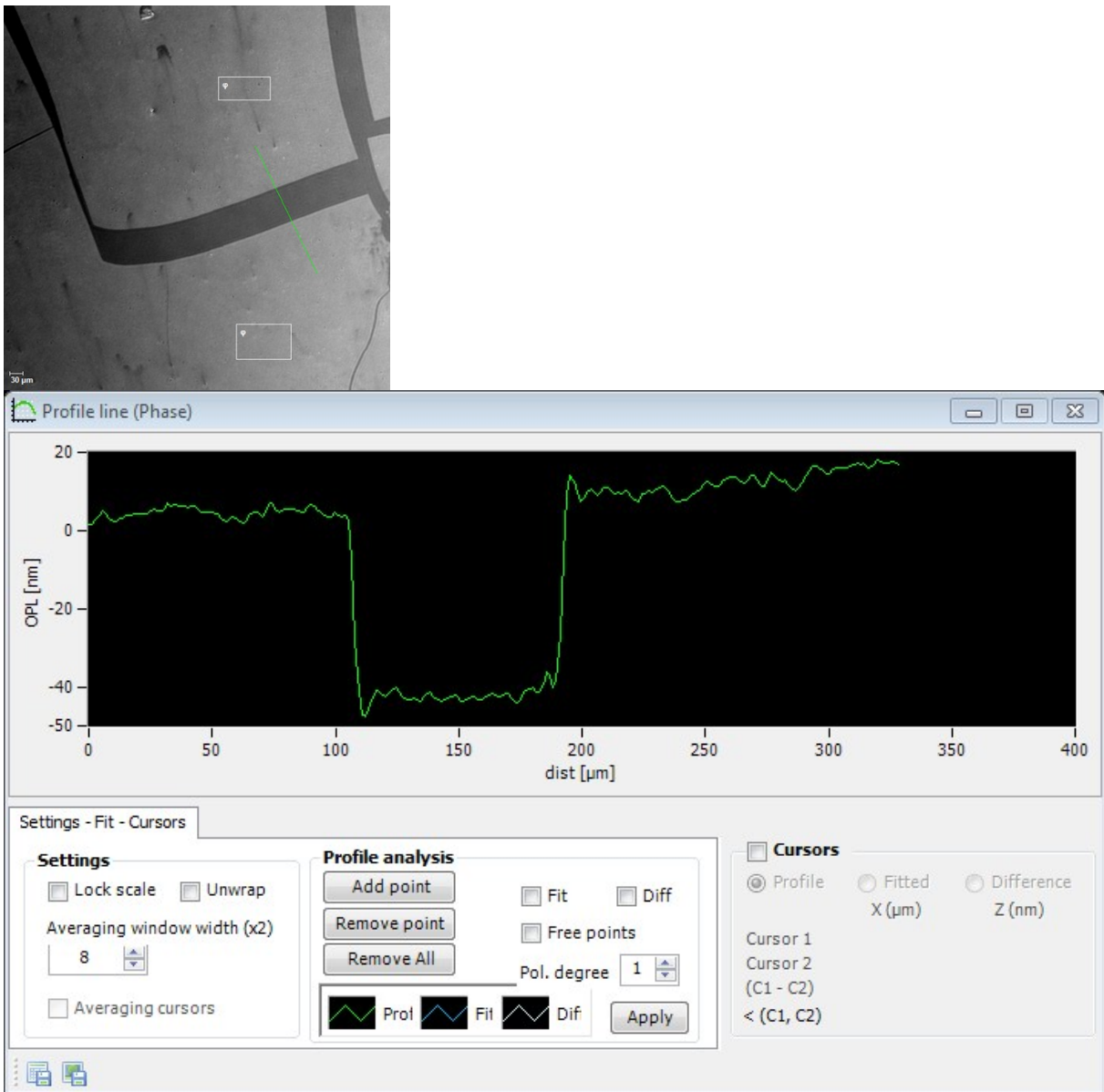


Figure S15 Evaluation of the hologram.

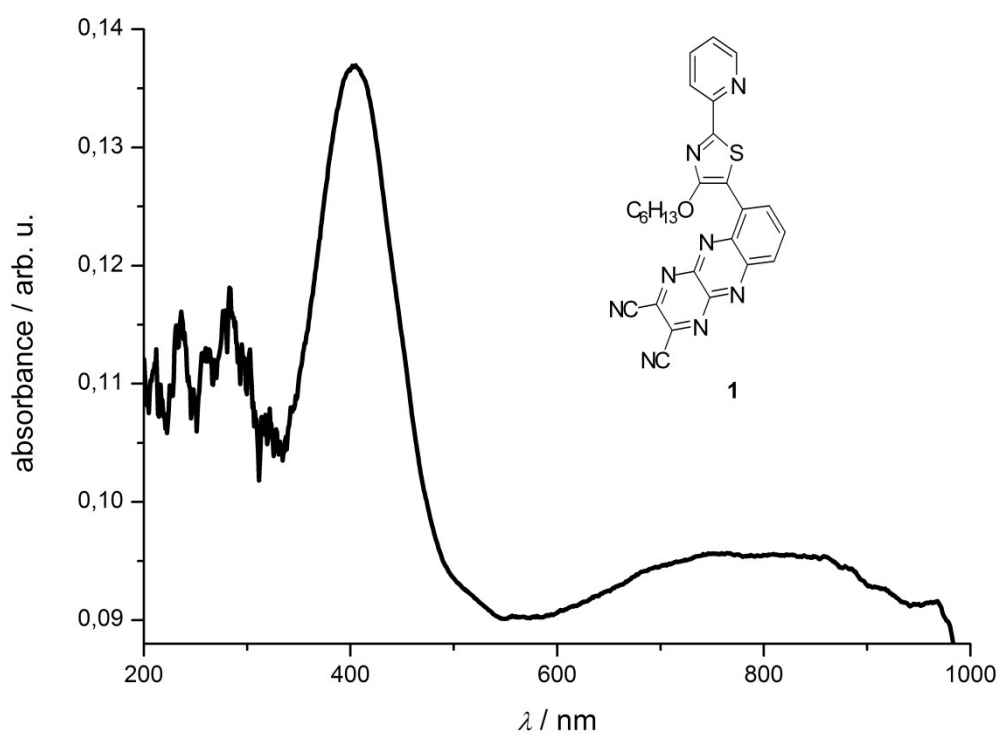


Figure S16 Film UV-vis of compound 1.

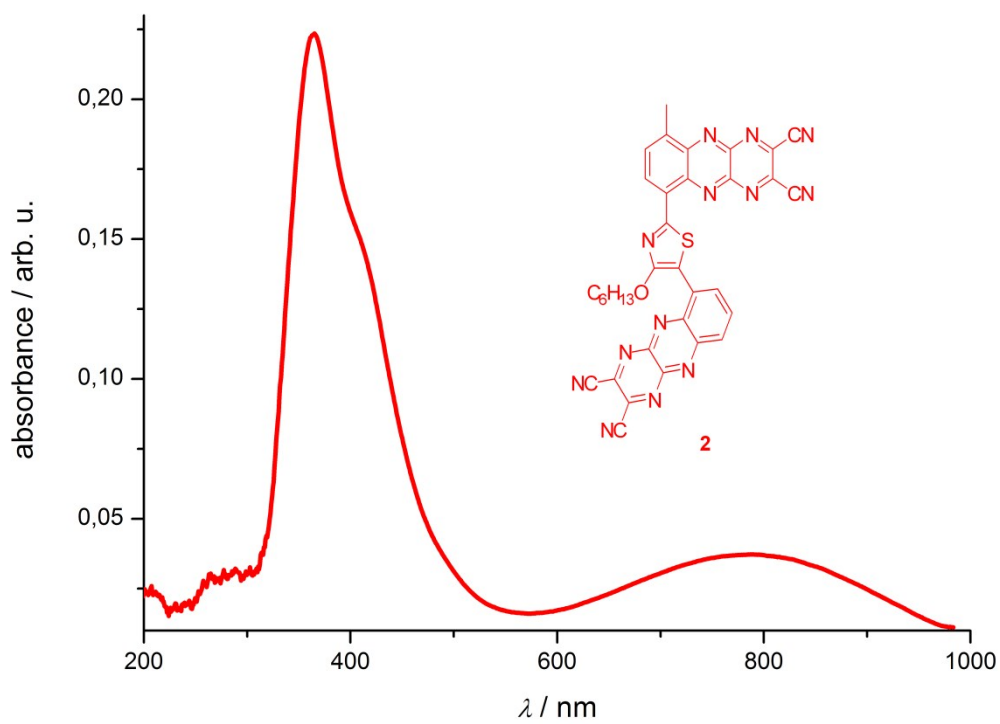


Figure S17 Film UV-vis of compound 2.

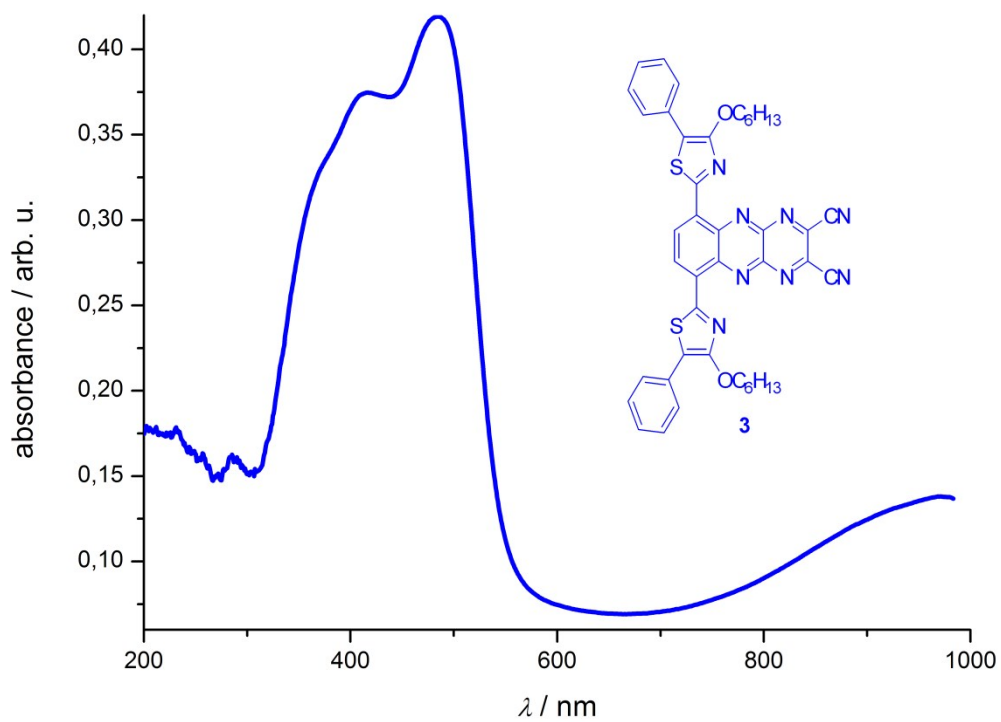


Figure S18 Film UV-vis of compound **3**.

2.5 DFT calculations

In order to gain more detailed insight into the electronic characteristics of the target compounds presented herein density functional theory (DFT) and time-dependent density functional theory (TD-DFT) calculations have been performed. The effects of solvation (THF) have been addressed by means of the polarizable continuum model.⁴ After an initial systematic conformational search with MMFF,⁵ the best geometries were optimized at the B3LYP/6-31+G(d,p)⁶ level of theory as implemented in Gaussian 09.⁷ After the ground state optimization and its validation via frequency calculation, the HOMO energies were calculated at B3LYP/6-31+G(d,p) while the LUMO energies were extracted from calculations at PBE/6-31+G(d,p) level of theory. Since the length of an alkyl-chain typically does not significantly influence the absorption and emission behaviour they were typically truncated for the reason of more economical calculations to methyl-groups.

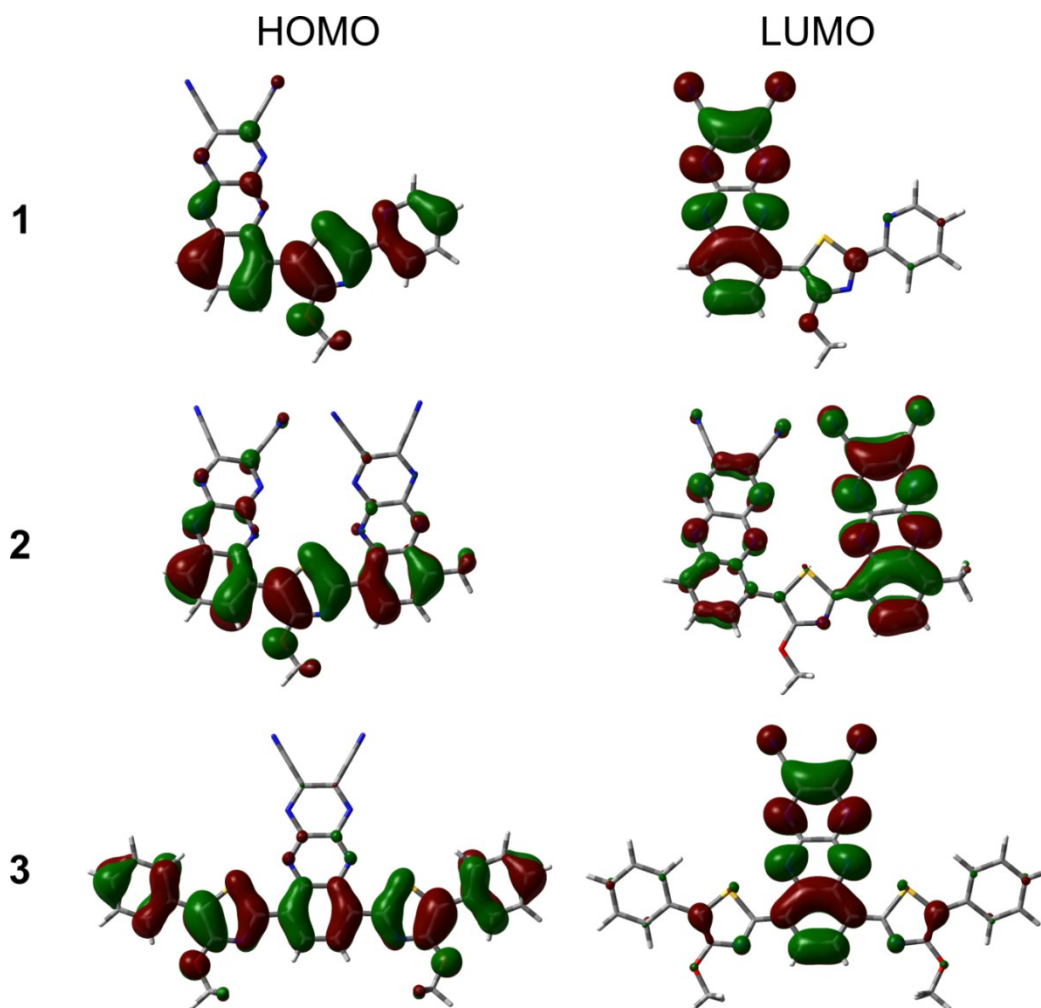


Figure S19 Graphical depiction of the frontier orbitals.

Coordinates

All optimized ground state structures showed no negative frequencies.

1

C	-5.9675390	2.9354780	0.0001350
C	-5.3230310	1.7002270	0.0001420
C	-3.9192910	1.6790880	0.0000270
N	-3.1714650	2.8005380	-0.0000430
C	-3.8049880	3.9771090	-0.0000460
C	-5.1986820	4.1009530	0.0000450
C	-3.1816630	0.4108460	-0.0000250
N	-3.7608830	-0.7731820	0.0001060
C	-2.8350240	-1.7608470	0.0000030
C	-1.4826910	-1.3799250	-0.0001660
S	-1.4431170	0.3826060	-0.0001570
O	-3.2254820	-3.0483540	0.0000310
C	-0.3127810	-2.2463840	-0.0001290
C	1.0412430	-1.7064410	0.0000490
C	2.1992650	-2.6103220	0.0001390
C	1.9962090	-4.0134930	0.0001780
C	0.7094590	-4.4939500	0.0000330
C	-0.4206940	-3.6359640	-0.0001590
N	1.2182680	-0.3908520	0.0000630
C	2.4720970	0.0833960	0.0001150
C	3.6042140	-0.8057100	0.0001430
N	3.4522650	-2.1317510	0.0001760
N	2.6333360	1.4316450	0.0001440
C	3.8685240	1.8830650	0.0001700
C	5.0083530	0.9922110	0.0000910
N	4.8767480	-0.3138340	0.0000680
C	-4.6412660	-3.3253090	-0.0002260
C	4.0591600	3.3114750	0.0000270
N	4.2267620	4.4614450	-0.0000240
C	6.3483600	1.5273220	-0.0001850
N	7.4224900	1.9700510	-0.0004040
H	-7.0519420	2.9870210	0.0001720
H	-5.8772130	0.7690670	0.0002210
H	-3.1728640	4.8618420	-0.0001110
H	-5.6596530	5.0829040	0.0000520
H	2.8627180	-4.6648320	0.0003120
H	0.5354050	-5.5655270	0.0000240
H	-1.4007160	-4.0887910	-0.0003270
H	-4.7146580	-4.4122030	-0.0004260
H	-5.1128280	-2.9100130	0.8931260
H	-5.1125590	-2.9096940	-0.8935700

2

C	4.7570190	-3.3484160	-0.9101120
C	3.3696630	-3.5399430	-0.6773100
C	2.5238020	-2.5071970	-0.3124460
C	3.1108430	-1.1985190	-0.1581280
C	4.5433070	-1.0098010	-0.4059230
C	5.3705780	-2.1212750	-0.7928830
N	2.3444180	-0.1779300	0.2210910
C	2.9211470	1.0210560	0.3619650
C	4.3230780	1.2098060	0.1021330
N	5.1074310	0.1944050	-0.2745280
N	2.1357400	2.0539250	0.7729320
C	2.7176490	3.2231210	0.9082810
C	4.1252240	3.4188160	0.6286530
N	4.9021890	2.4356560	0.2382900
C	1.1010840	-2.7855900	-0.0935450
N	0.6532080	-4.0326260	-0.0932820
C	-0.6833490	-4.0796010	0.0802000
C	-1.3579330	-2.8553680	0.2016660
S	-0.1493160	-1.5836560	0.0941250
O	-1.3215920	-5.2640810	0.1247130
C	-2.7787760	-2.6410000	0.4389220
C	-3.3970030	-1.3347390	0.2602680
C	-4.8325650	-1.1591640	0.5107660
C	-5.6162140	-2.2685130	0.9217800
C	-5.0064380	-3.4892130	1.0759840
C	-3.6187550	-3.6755720	0.8410830
N	-2.6535260	-0.3098990	-0.1417040
C	-3.2503540	0.8785470	-0.3079350
C	-4.6558890	1.0505320	-0.0475850
N	-5.4224690	0.0349090	0.3561260
N	-2.4822070	1.9114730	-0.7422650
C	-3.0804790	3.0709500	-0.9033580
C	-4.4897340	3.2503100	-0.6272790
N	-5.2524400	2.2661930	-0.2124080
C	6.8369030	-1.9201610	-1.0501290
C	-0.5395630	-6.4582450	-0.0782410
C	4.7222890	4.7233450	0.7775060
N	5.1932100	5.7781010	0.9017270
C	1.9064820	4.3257060	1.3618880
N	1.2666850	5.2206750	1.7354140
C	-2.2846110	4.1738340	-1.3802380
N	-1.6556250	5.0688960	-1.7722170
C	-5.1071780	4.5418500	-0.8078160
N	-5.5942210	5.5858720	-0.9578790
H	5.3489400	-4.2119890	-1.1982780
H	2.9512030	-4.5326190	-0.7953670
H	-6.6742250	-2.1178480	1.1037030
H	-5.5907790	-4.3472170	1.3935290
H	-3.2055720	-4.6629750	0.9884860
H	7.3075680	-2.8624470	-1.3386740
H	6.9995470	-1.1875870	-1.8474650
H	7.3431630	-1.5326830	-0.1598540
H	-1.2545900	-7.2776090	-0.0132880
H	-0.0649490	-6.4429730	-1.0622110
H	0.2233800	-6.5537800	0.6976400

3

C	0.7027980	-2.4787510	-0.0066310
C	-0.7028580	-2.4787740	-0.0087670
C	-1.4592800	-1.3102180	-0.0149250
C	-0.7345360	-0.0656140	-0.0238050
C	0.7344710	-0.0655590	-0.0162140
C	1.4592100	-1.3101690	-0.0079520
N	-1.4098170	1.0817260	-0.0416290
C	-0.7184440	2.2263670	-0.0478560
C	0.7183840	2.2264950	-0.0313970
N	1.4097510	1.0819180	-0.0181970
N	-1.4218600	3.3908310	-0.0717670
C	-0.7237080	4.5037730	-0.0739680
C	0.7236830	4.5039870	-0.0480620
N	1.4218190	3.3911980	-0.0289270
C	2.9143920	-1.3954850	-0.0025580
C	-2.9144650	-1.3955010	-0.0115510
N	3.5310620	-2.5681750	0.0026520
C	4.8750770	-2.4340130	0.0044070
C	5.3812100	-1.1322010	0.0087100
S	4.0185460	-0.0378670	-0.0057270
S	-4.0185540	-0.0378270	-0.0138300
C	-5.3812310	-1.1320630	0.0066780
C	-4.8751860	-2.4339100	0.0016070
N	-3.5311870	-2.5681500	-0.0037580
C	6.7633010	-0.6522830	0.0280320
C	-6.7631940	-0.6520450	0.0315910
O	-5.6778530	-3.5196650	0.0148720
O	5.6777290	-3.5198120	0.0144370
C	7.8438540	-1.5014390	-0.3001210
C	9.1547290	-1.0233580	-0.2880870
C	9.4270040	0.3062910	0.0471610
C	8.3671410	1.1592500	0.3739580
C	7.0559150	0.6880040	0.3671460
C	-7.0541990	0.6882780	0.3719720
C	-8.3653850	1.1594810	0.3851390
C	-9.4268010	0.3064280	0.0636770
C	-9.1561160	-1.0232130	-0.2728840
C	-7.8452910	-1.5012370	-0.2913260
C	-5.0487740	-4.8128120	0.0665990
C	5.0487200	-4.8130480	0.0646700
C	1.4512680	5.7488690	-0.0414780
N	2.0262530	6.7584580	-0.0355380
C	-1.4512930	5.7483090	-0.1035100
N	-2.0263080	6.7576150	-0.1274220
H	1.2242430	-3.4285100	-0.0021770
H	-1.2242900	-3.4285420	-0.0046410
H	7.6511380	-2.5323090	-0.5675890
H	9.9673740	-1.6962570	-0.5466200
H	10.4489630	0.6730670	0.0553020
H	8.5611320	2.1938730	0.6412680
H	6.2531420	1.3667770	0.6395940
H	-6.2501370	1.3671060	0.6404440
H	-8.5581180	2.1940950	0.6533950
H	-10.4487350	0.6731260	0.0769400
H	-9.9699960	-1.6961520	-0.5273930
H	-7.6538450	-2.5321260	-0.5596280
H	-5.8705660	-5.5282890	0.0799880
H	-4.4201350	-4.9728170	-0.8131080
H	-4.4439350	-4.9125940	0.9717340
H	5.8705270	-5.5285500	0.0754410
H	4.4452200	-4.9145710	0.9704910
H	4.4187710	-4.9713590	-0.8144210

3. Attachment

3.1 X-ray analysis

Crystal Structure Determination

The intensity data were collected on a Nonius KappaCCD diffractometer, using graphite-monochromated Mo-K α radiation. Data were corrected for Lorentz and polarization effects; absorption was taken into account on a semi-empirical basis using multiple-scans.⁸⁻¹⁰

The structure was solved by direct methods (SHELXS)¹¹ and refined by full-matrix least squares techniques against Fo² (SHELXL-97).¹¹ The hydrogen atoms were located by difference Fourier synthesis and refined isotropically. Only the the carbon atoms C20B, C7C and C20C the hydrogen atom positions were included at calculated positions with fixed thermal parameters. XP¹² was used for structure representations.

Crystal Data for 11: C₂₀H₂₀N₄OS₂, Mr = 396.52 g mol⁻¹, light_yellow prism, size 0.122 x 0.108 x 0.096 mm³, monoclinic, space group P 2₁/c, a = 18.3460(4), b = 13.6120(3), c = 23.8450(5) Å, β = 104.844(1)°, V = 5756.0(2) Å³, T = -140 °C, Z = 12, $\rho_{\text{calcd.}}$ = 1.373 g cm⁻³, μ (Mo-K α) = 2.95 cm⁻¹, multi-scan, transmin: 0.6500, transmax: 0.7456, F(000) = 2496, 67584 reflections in h(-23/23), k(-17/17), l(-29/30), measured in the range 1.89° ≤ Θ ≤ 27.56°, completeness Θ_{max} = 99.4%, 13218 independent reflections, R_{int} = 0.0481, 10486 reflections with F_o > 4 σ (F_o), 944 parameters, 0 restraints, R1_{obs} = 0.0738, wR²_{obs} = 0.1595, R1_{all} = 0.0960, wR²_{all} = 0.1725, GOOF = 1.135, largest difference peak and hole: 0.942 / -0.486 e Å⁻³.

Supporting Information Available: Crystallographic data deposited at the Cambridge

Crystallographic Data Centre under CCDC-1554777 for **11** contain the supplementary crystallographic data excluding structure factors; this data can be obtained free of charge via

www.ccdc.cam.ac.uk/conts/retrieving.html (or from the Cambridge Crystallographic Data Centre, 12, Union Road, Cambridge CB2 1EZ, UK; fax: (+44) 1223-336-033; or deposit@ccdc.cam.ac.uk).

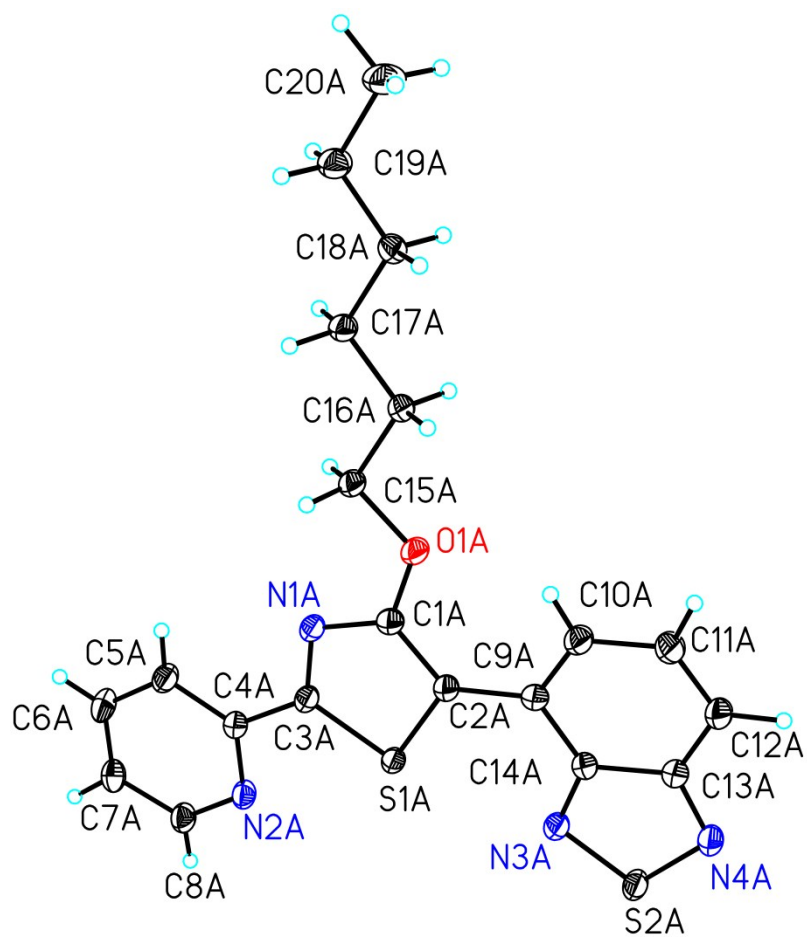


Figure S20 ORTEP view of structure **11**. The hydrogen atoms are omitted for clarity and thermal ellipsoids at a 50% probability level.

3.2 NMR spectra

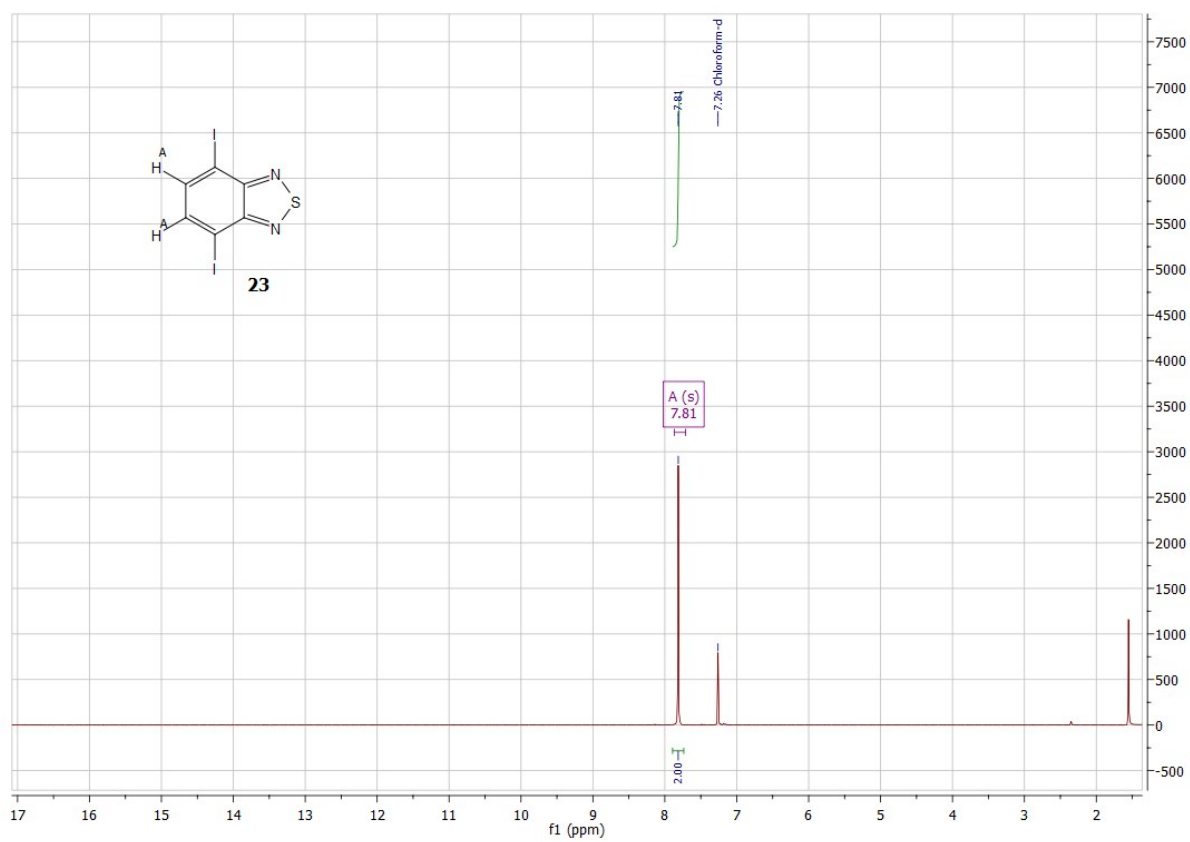


Figure S21 ^1H NMR of **23**.

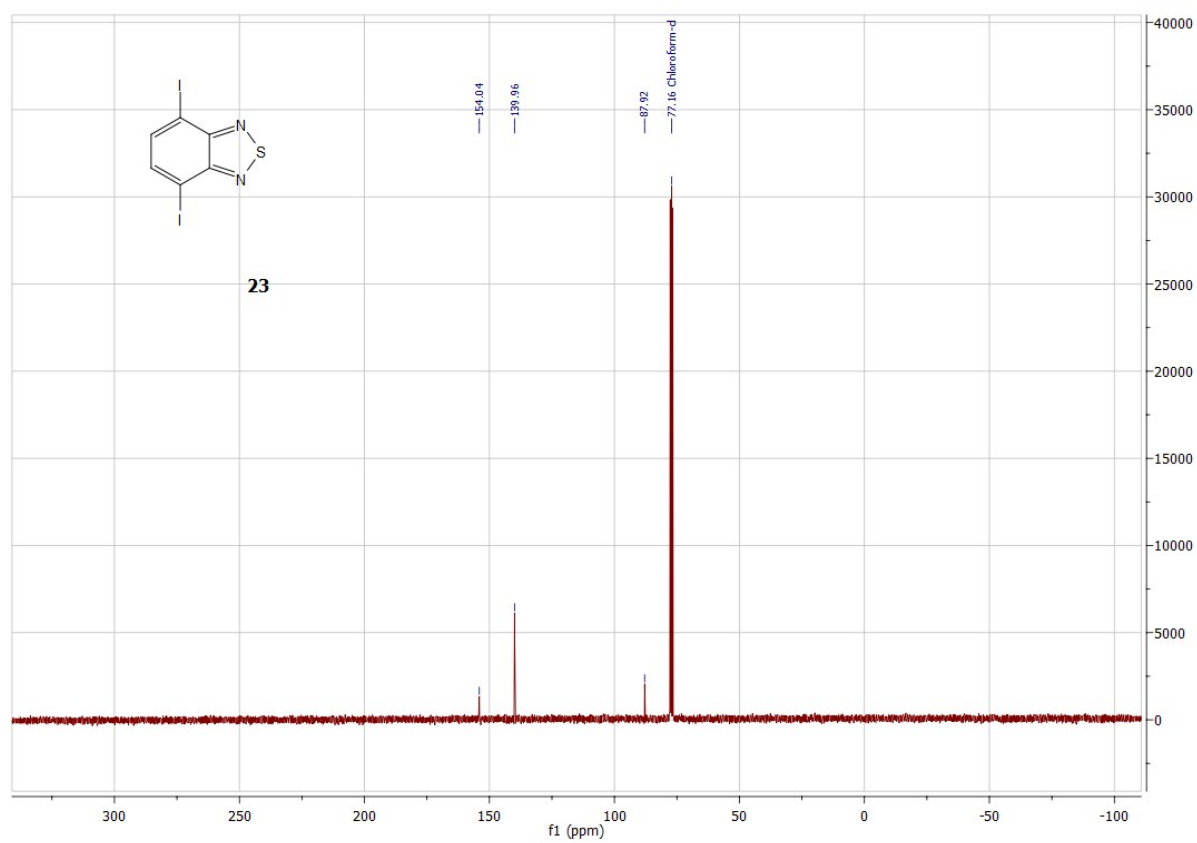


Figure S22 ^{13}C NMR of **23**.

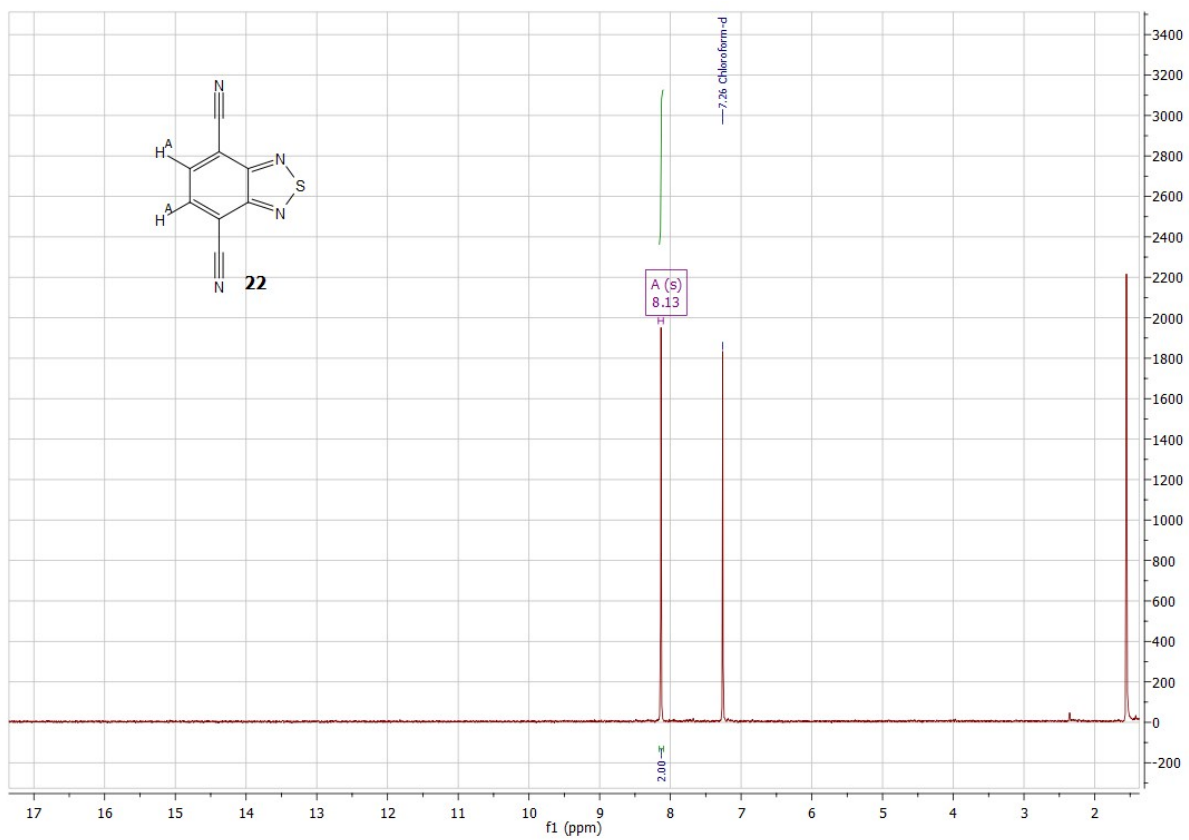


Figure S23 ^1H NMR of **22**.

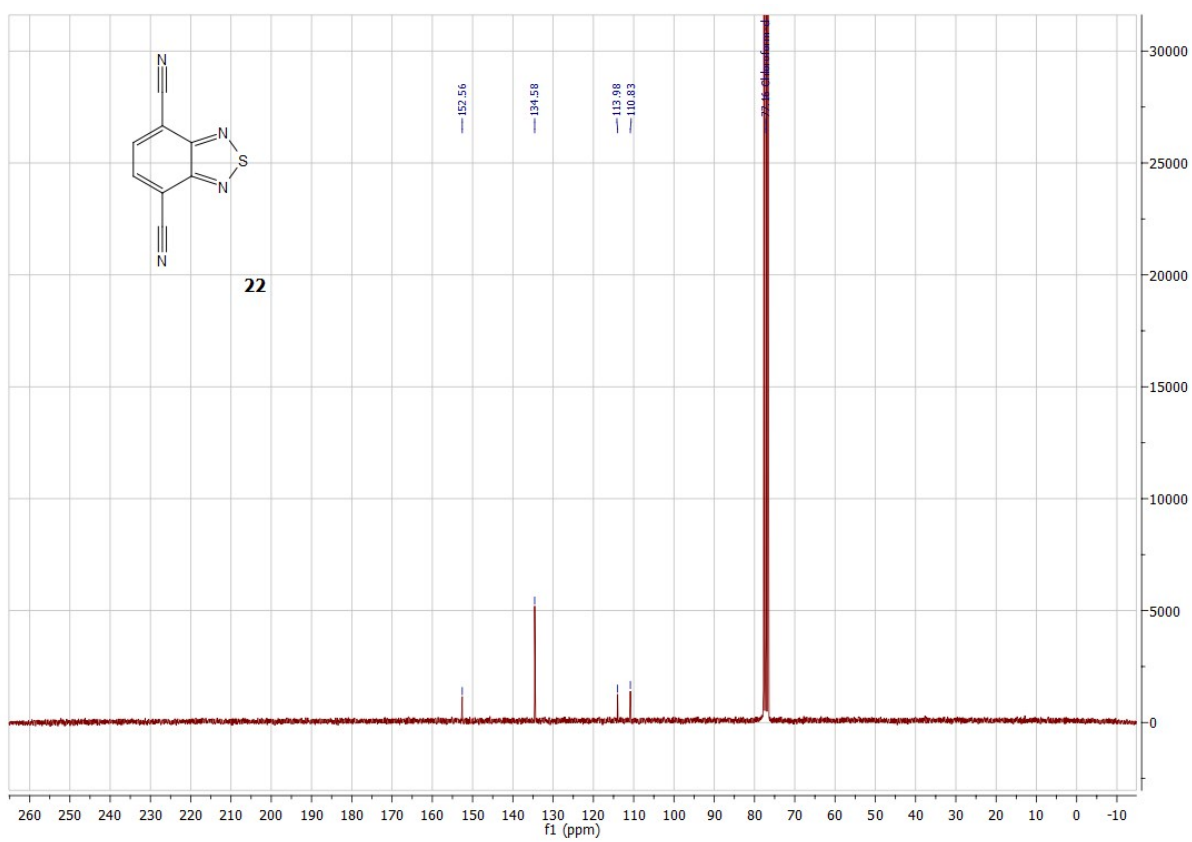


Figure S24 ^{13}C NMR of **22**.

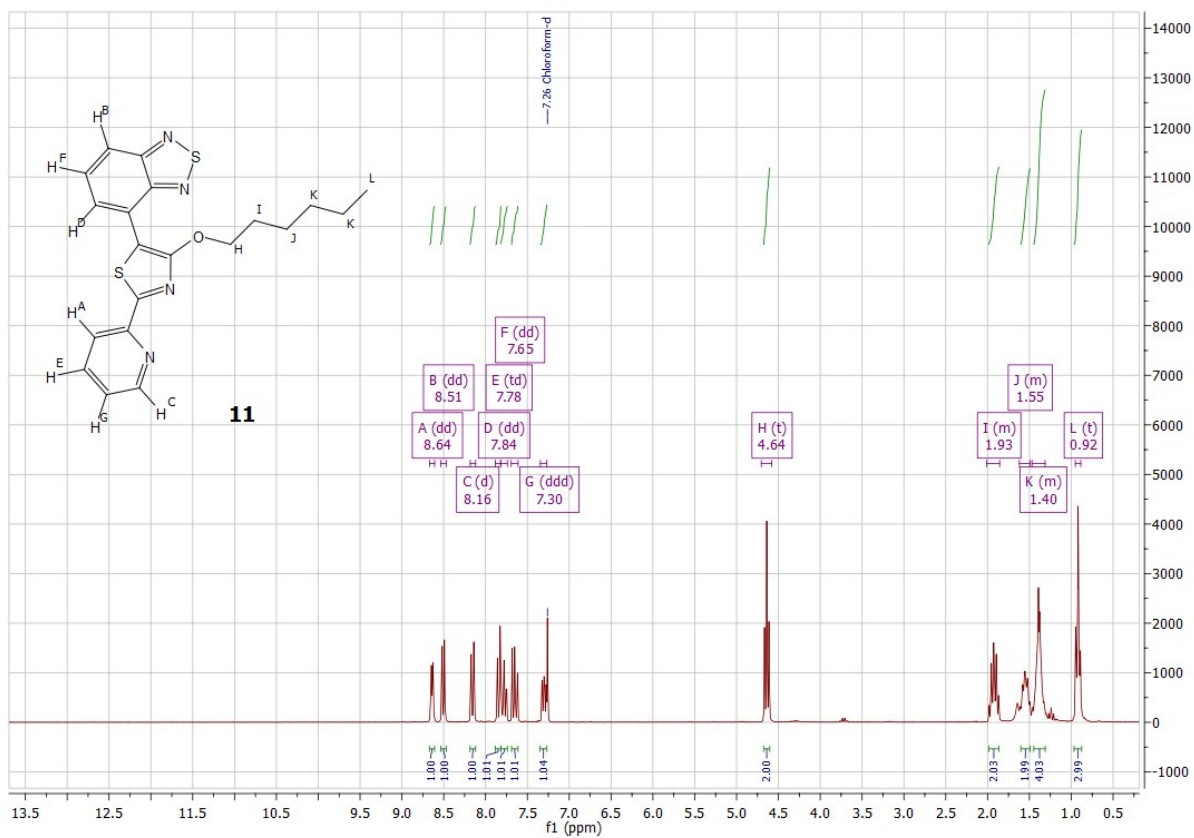


Figure S25 ¹H NMR of **11**.

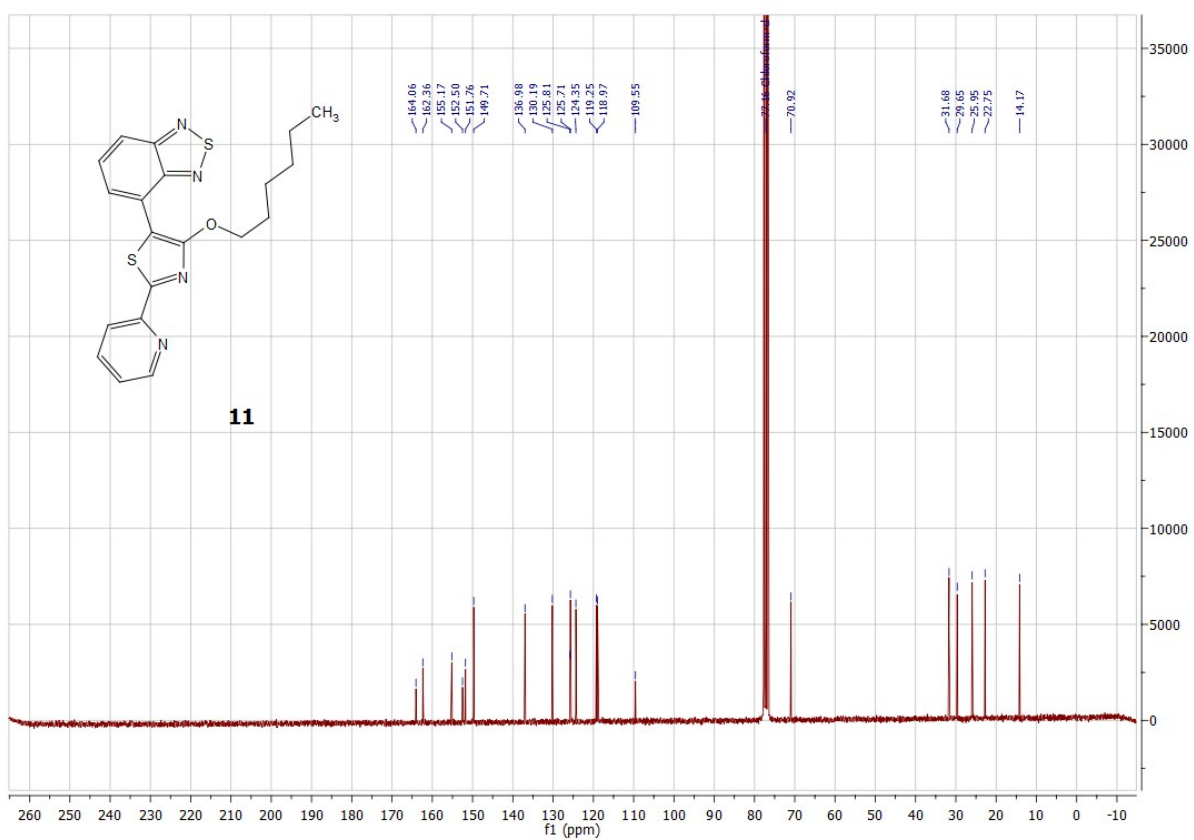


Figure S26 ¹³C NMR of **11**.

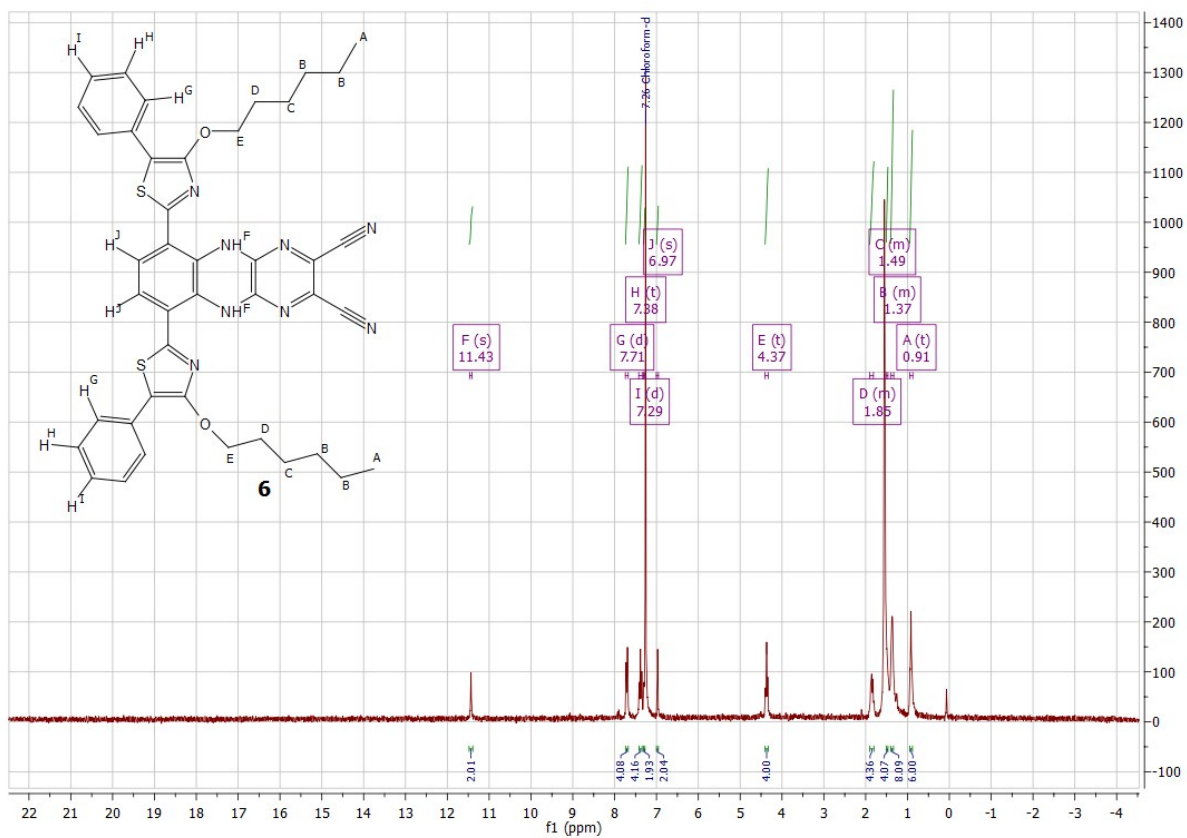


Figure S27 ^1H NMR of **6**.

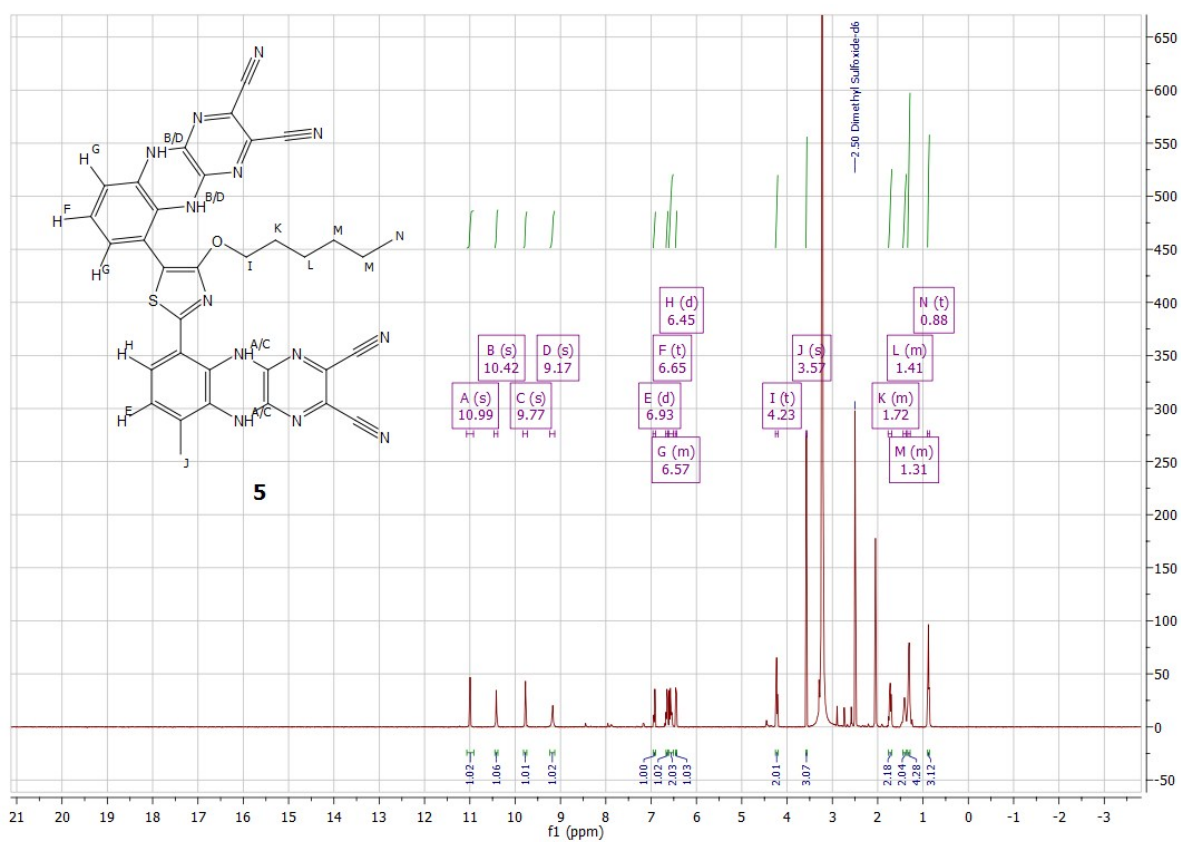


Figure S28 ^1H NMR of **5**.

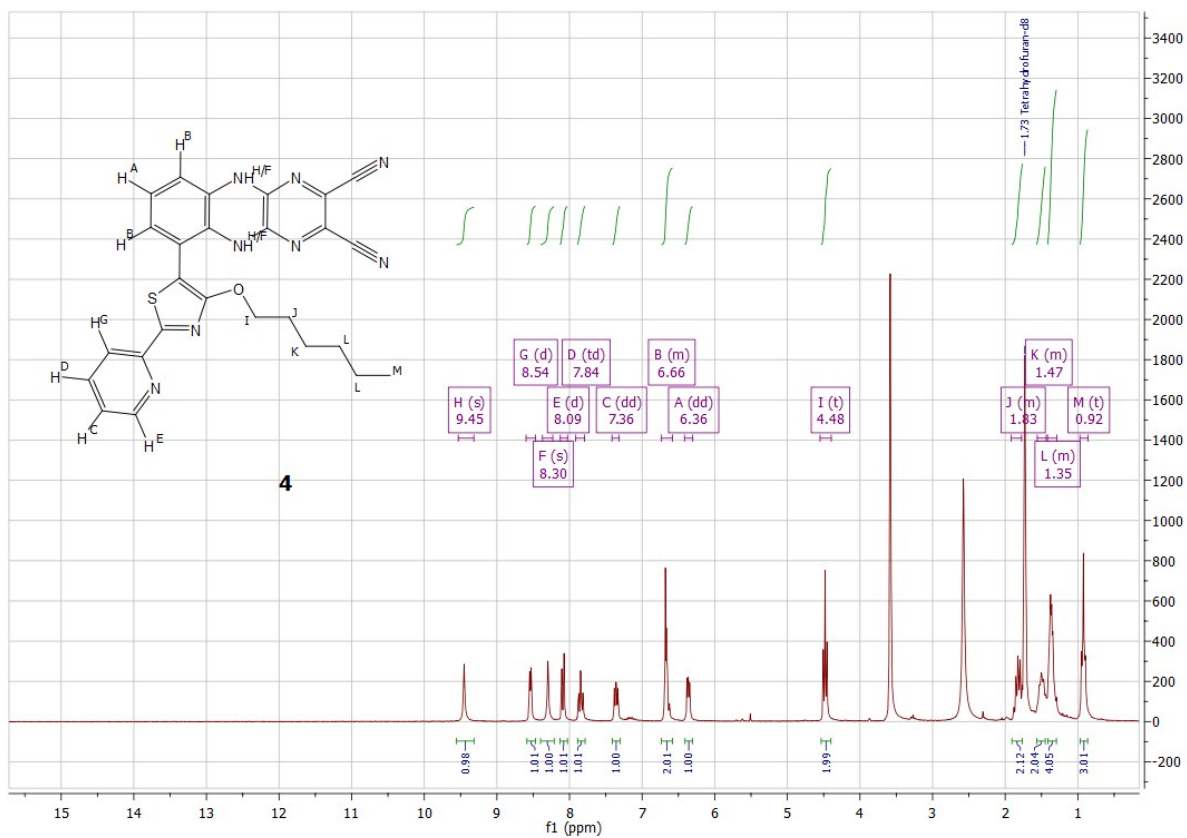


Figure S29 ^1H NMR of **4**.

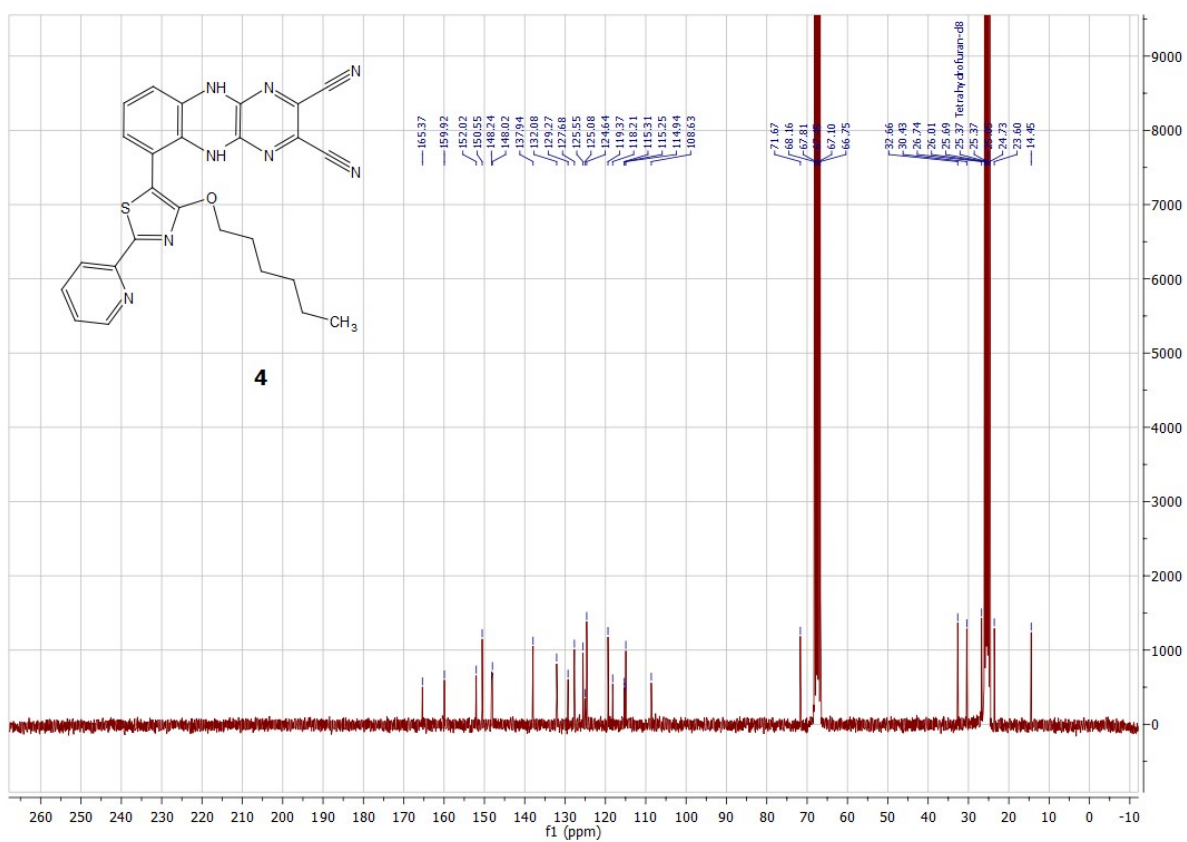


Figure S30 ^{13}C NMR of **4**.

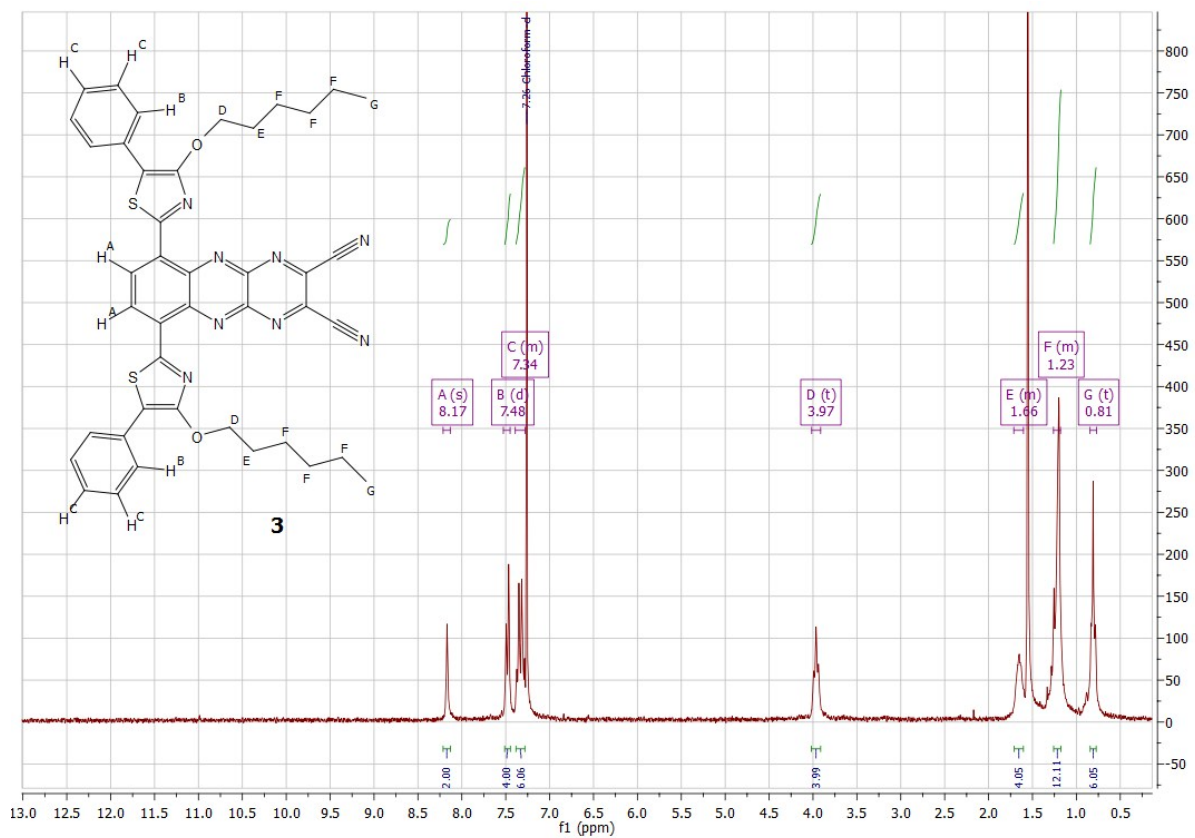


Figure S31 ^1H NMR of **3**.

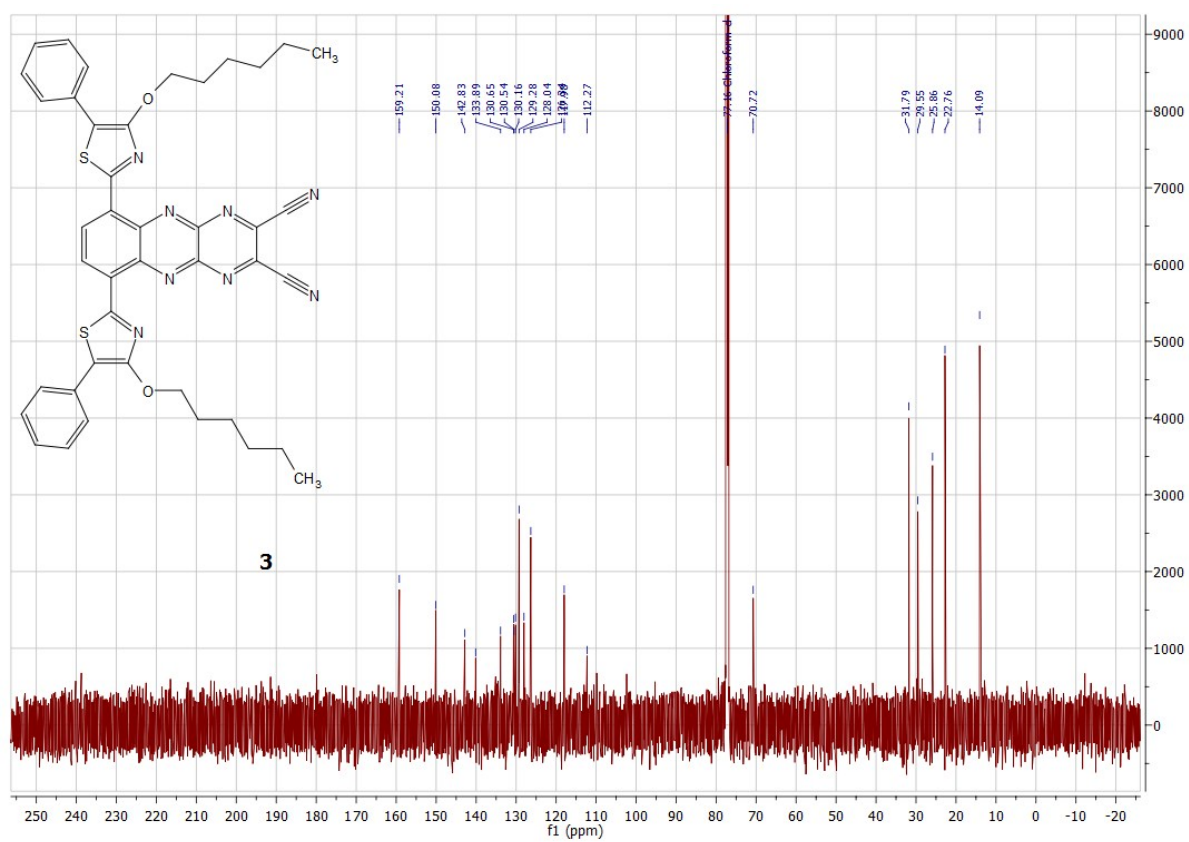


Figure S32 ^{13}C NMR of **3**.

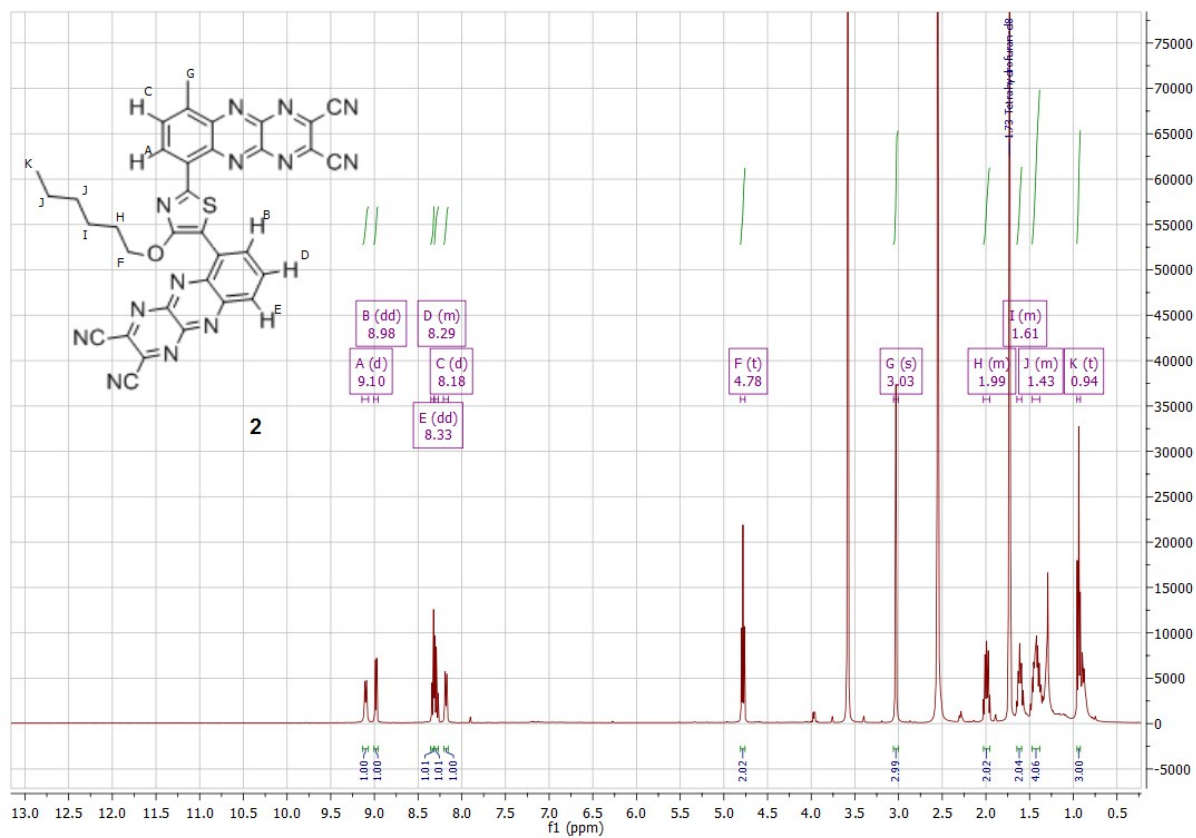


Figure S33 ^1H NMR of **2**.

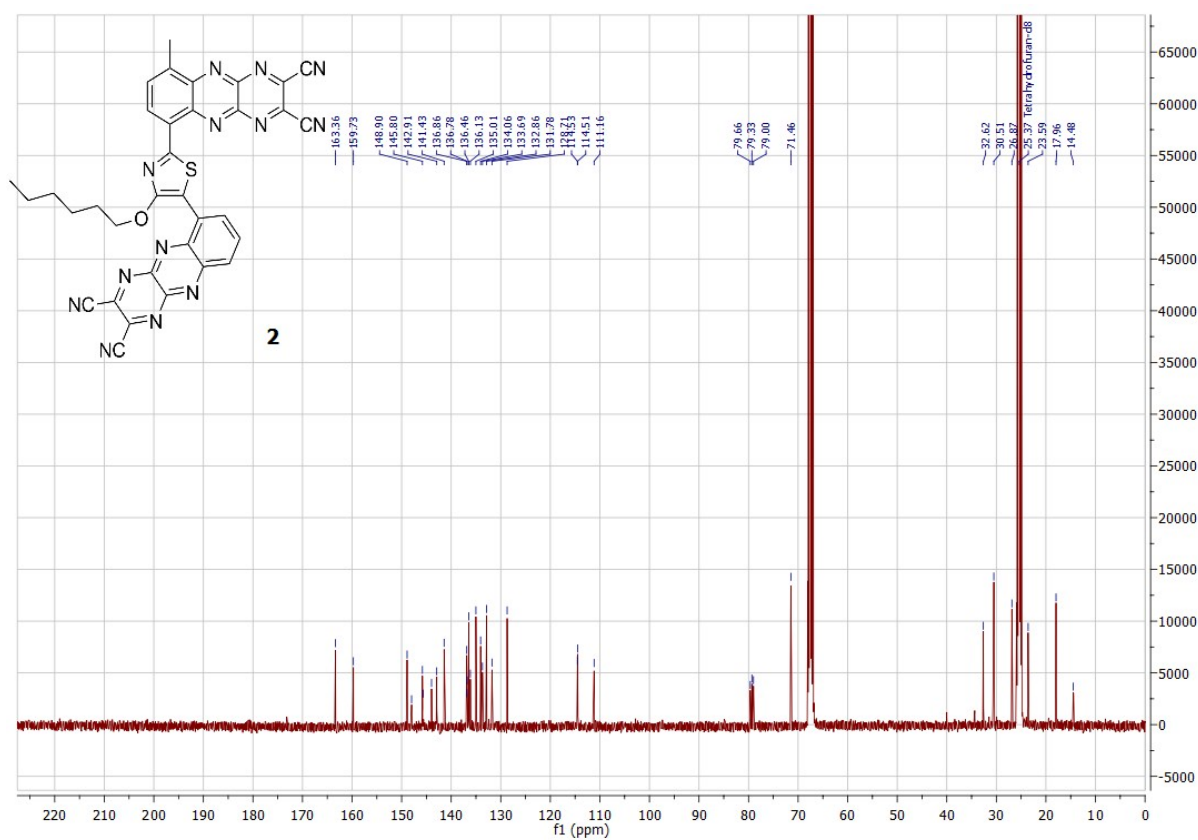


Figure S34 ^{13}C NMR of **2**.

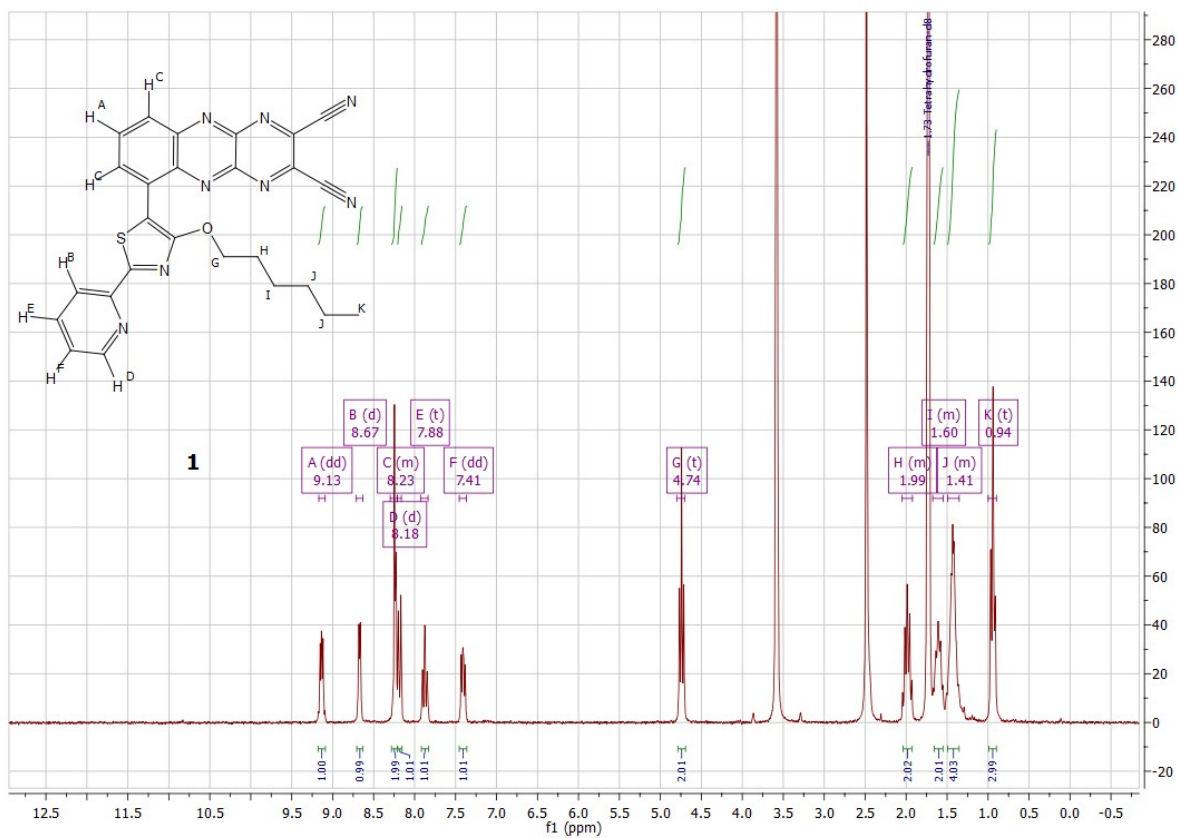


Figure S35 ^1H NMR of **1**.

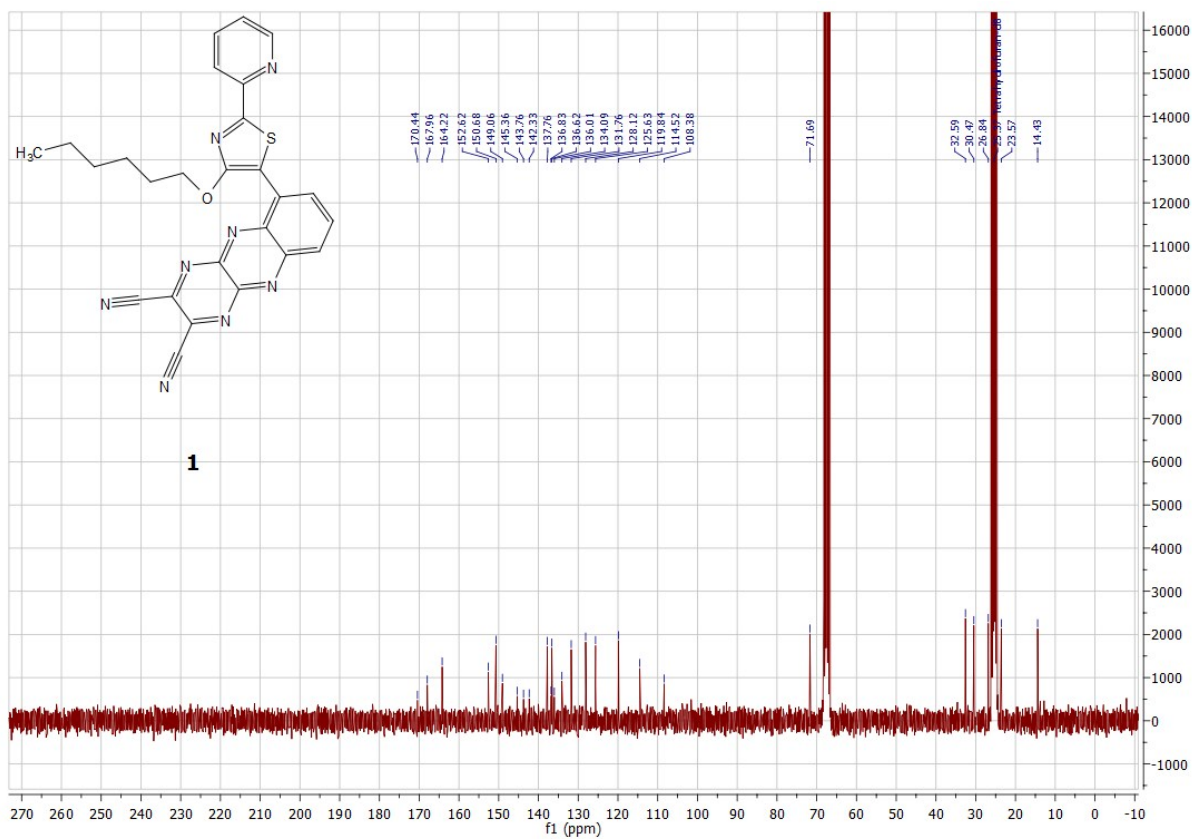


Figure S36 ^{13}C NMR of **1**.

4. References

1. (a) S. Fery-Forgues, Lavabre, D., *J. Chem. Educ.*, 1999, **76**, 1260; (b) A. M. Brouwer, *Pure Appl. Chem.*, 2011, **83**, 2213.
2. D. M. Gampe, F. Nöller, V. G. Hänsch, S. Schramm, A. Darsen, S. H. Habenicht, S. Ehrhardt, D. Weiß, H. Görls and R. Beckert, *Tetrahedron*, 2016, **72**, 3232.
3. N. Cho, K. Song, J. K. Lee and J. Ko, *Chem. Eur. J.*, 2012, **18**, 11433.
4. J. Tomasi, B. Mennucci and R. Cammi, *Chem. Rev.*, 2005, **105**, 2999.
5. T. A. Halgren, *J. Comput. Chem.*, 1996, **17**, 490.
6. T. Yanai, D. P. Tew and N. C. Handy, *Chem. Phys. Lett.*, 2004, **393**, 51.
7. M. J. Frisch, G. W. Trucks, H. B. Schlegel, G. E. Scuseria, M. A. Robb, J. R. Cheeseman, G. Scalmani, V. Barone, B. Mennucci, G. A. Petersson, H. Nakatsuji, M. Caricato, X. Li, H. P. Hratchian, A. F. Izmaylov, J. Bloino, G. Zheng, J. L. Sonnenberg, M. Hada, M. Ehara, K. Toyota, R. Fukuda, J. Hasegawa, M. Ishida, T. Nakajima, Y. Honda, O. Kitao, H. Nakai, T. Vreven, J. A. Montgomery Jr., J. E. Peralta, F. Ogliaro, M. J. Bearpark, J. Heyd, E. N. Brothers, K. N. Kudin, V. N. Staroverov, R. Kobayashi, J. Normand, K. Raghavachari, A. P. Rendell, J. C. Burant, S. S. Iyengar, J. Tomasi, M. Cossi, N. Rega, N. J. Millam, M. Klene, J. E. Knox, J. B. Cross, V. Bakken, C. Adamo, J. Jaramillo, R. Gomperts, R. E. Stratmann, O. Yazyev, A. J. Austin, R. Cammi, C. Pomelli, J. W. Ochterski, R. L. Martin, K. Morokuma, V. G. Zakrzewski, G. A. Voth, P. Salvador, J. J. Dannenberg, S. Dapprich, A. D. Daniels, Ö. Farkas, J. B. Foresman, J. V. Ortiz, J. Cioslowski and D. J. Fox, *Gaussian 09, Revision A.02*, Gaussian, Inc., Wallingford, CT, 2009.
8. COLLECT, Data Collection Software; Nonius B.V., Netherlands, 1998.
9. Z. Otwinowski and W. Minor, *Methods Enzymol.* 1997, **276** (Ed.: Charles W. Carter Jr.), 307.
10. SADABS 2.10, Bruker-AXS inc., 2002, Madison, WI, U.S.A.
11. G. Sheldrick, *Acta Crystallogr., Sect. A*, 2008, **64**, 112.
12. Siemens (1994). XP. Siemens Analytical X-ray Instruments Inc., Madison, Wisconsin, USA.